Elucidation of Mechanism of Death-associated Protein Kinase-2 (DAPK2)-induced Apoptosis

Kinuka Isshiki

Depertment of Biological Science and Technology,

Faculty of Engineering,

Tokushima University

March 2016

CONTENTS

Chapter 1. General Introduction 1

1.1. Cancer and anti-cancer agents 1

1.2. Apoptosis 2

1.3. The death-associated protein kinase (DAPK) family 4

1.4. cGMP-dependent protein kinase I (cGK-I) 7

1.5. Tubulin and microtubule 9

Chapter 2. Mechanism of DAPK2 regulation 10

2.1. Introduction 10

2.2. Materials and methods 10

2.2.1. Plasmid construction 10

2.2.2. Cell culture and transfection 11

2.2.3. Protein microarray 11

2.2.4. *In vitro* kinase assay 12

2.2.5. Analysis of apoptosis 13

2.3. Results 13

2.3.1. Identification of putative substrates for cGK-I by protein microarray analysis 13

2.3.2. cGK-Ib phosphorylates DAPK2 at Ser^{299}, Ser^{367} and Ser^{368} 16

2.3.3. Phosphorylation of DAPK2 at Ser^{299} by cGK-I increases its kinase activity 17

2.3.4. A phospho-mimic mutant DAPK2 S299D strongly induces apoptosis compared with wild-type DAPK2 20

2.4. Discussion 21

Chapter 3. Mechanism of apoptosis induction 24

3.1. Introduction 24

3.2. Materials and methods 24

3.2.1. Antibodies 24

3.2.2. Plasmid construction 24

3.3.3. Cell culture, transfection and RNA interference 25

3.3.4. Protein identification by matrix-assisted laser desorption/ionization time-of-flight mass spectrometry (MALDI-TOF MS) 25

3.3.5. Co-immunoprecipitation and pull-down assays 27

3.3.6. Apoptotic cell death assay 27
3.3. Results 27
3.3.1. Identification of β-tubulin as a novel binding partner to DAPK2 27
3.3.2. β-Tubulin interacts with monomeric but not dimeric DAPK2 32
3.3.3. Role of DAPK2 in nocodazole-induced apoptosis 34
3.4. Discussion 36
Chapter 4. Summary 39
Chapter 5. Acknowledgment 41
Chapter 6. References 42
Chapter 7. Appendix 50

Abbreviation

cGK	cGMP-dependent protein kinase
DAPK	death-associated protein kinase
TNF	tumor necrosis factor
IFN	interferon
NO	nitric oxide
CaM	Calmodulin
MLC	myosin light chain
GST	glutathione S-transferase
GFP	green fluorescent protein
MALDI-TOF MS	matrix-assisted laser desorption/ionization time-of-flight mass spectrometry
PARP	poly (ADP-ribose) polymerase
PCD	programmed cell death
Pin1	peptidyl-prolyl isomerase, protein NIMA-interacting 1

Chapter 1. General Introduction

1.1. Cancer and anti-cancer agents

Cancer has been a one of worldwide fame cause of death. In developing countries, infectious diseases including malaria and tuberculosis still have had the majority of cause of death. On the other hand, cancer, cerebrovascular disease and heart disease, that are called “three major diseases”, make up most of it in developed countries. In Japan, in age-adjusted death rate, cerebrovascular and heart diseases have been decreasing [2010 Specified Report of Vital Statistics Statistical Surveys conducted by Ministry of Health, Labour and Welfare (Japan)]. However, the age-adjusted death rate of cancer has been walking sideways. It is showed that therapy of cancer didn't have a big improvement. Thus, development of cancer therapy is expected.

Chemotherapy (treatment with anti-cancer agent) is a one of cancer therapy. Anti-cancer agents are roughly classified into the following group; cytotoxic drug, cell biological modifier (such as growth inhibitor) and biological response modifier (such as cytokine) [1]. Of these, cytotoxic drugs are primary anti-cancer agents. Mechanisms of these agents are many and varied. For example, paclitaxel that belongs to the plant alkaloid family, causes dysregulation of microtubule and results in apoptosis induction [2]. In this way, cell death including apoptosis is an important target of anti-cancer agent.

1.2. Apoptosis

Apoptosis is essential roles to provide for many physiological phenomenon, such as development, maintenance of homeostasis and immunoresponce. Dysregulation of apoptosis causes cancer[3]. Cancer cells are hard to cause apoptosis. Thus, in cancer therapy, it is important how to induce apoptosis in cancer cells [3]. In fact, molecular biological research of apoptosis in mammal makes progress in cancer field. B-cell lymphoma 2 (Bcl-2), was the first identified apoptosis-associated factor in mammal, was identified as an oncogene in the 1980's [4, 5]. Further, apoptosis-associated factors are often oncogenes (Bcl-2, for example) [4, 5] or cancer suppressor genes (p53, for example) [6].

Apoptosis is a one of programmed cell death (PCD), and is defined as activation of cysteine protease "caspase". Caspase cascade is the basis of apoptosis. Apoptosis is caused by endogenous factors such as DNA damage and endoplasmic reticulum (ER) stress, and exogenous factors such as death signals from death receptors. The endogenous apoptosis signals mainly induce apoptosis via mitochondria. These apoptosis signals inhibit anti-apoptosis protein Bcl-2, and release cytochrome c from mitochondria. Cytochrome c activates caspase-9 and active-caspase-9 activates caspase-3. Active-caspase-3 cleaves various substrates including poly-ADP ribose polymerase (PARP), and results in cell death (Fig.1) [7]. In exogenous death receptor signaling, caspase-8 that is activated by binding ligand to receptor activates caspase-3. However, apoptosis signaling is not only these. The signaling causes crosstalk with other signalings such as survival signals, autophagy, cell adhesion and cell cycle. For example, in cell cycle, the cells that do not transit cell cycle checkpoints cause apoptosis [8]. Paclitaxel targets to this signal. This drug

inhibits regulation of mitotic apparatus via dysregulation of microtubule, results in cell cycle arrest and apoptosis induction [9]. But, the mechanisms of crosstalk between apoptosis signal and other signals are not fully revealed.

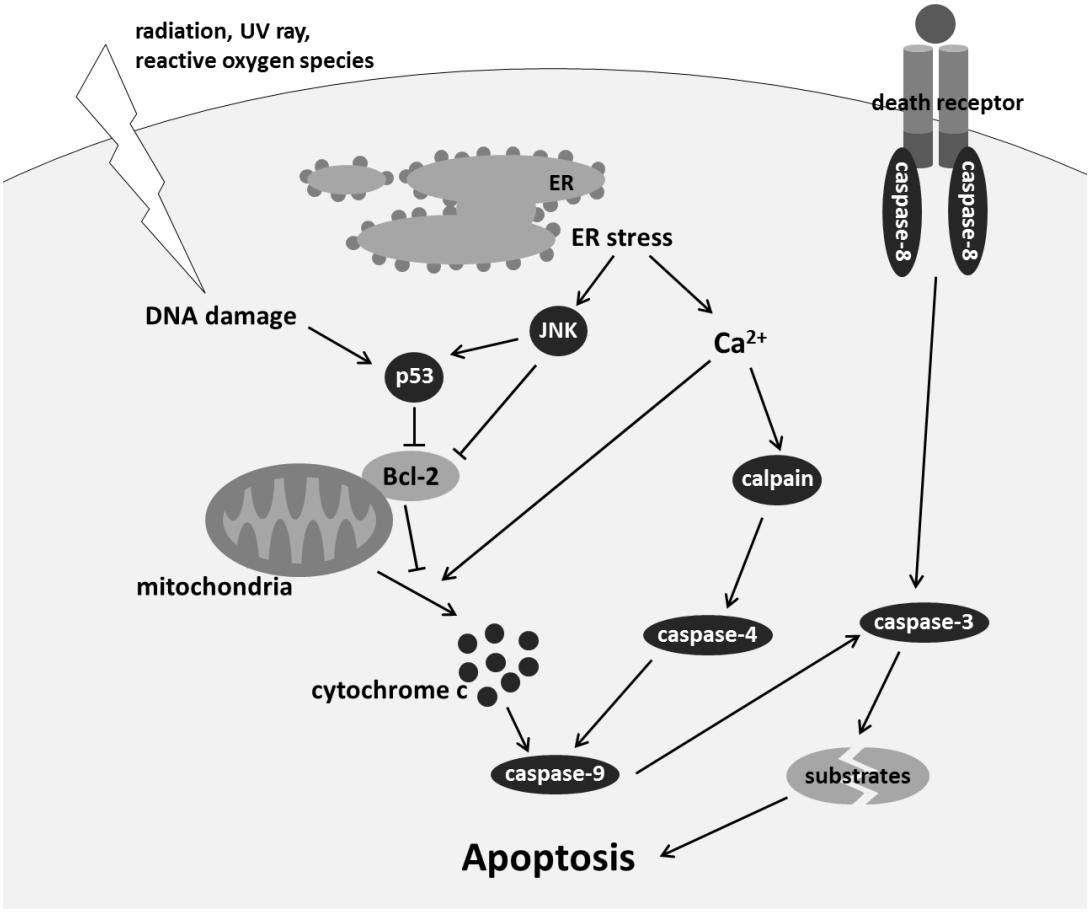

Fig.1 Apoptosis cascades

1.3. The death-associated protein kinase (DAPK) family

The DAPK family consists of five members: DAPK1 [10], DAPK2 (DRP-1) [11], DAPK3 (ZIPK/DLK) [12], DRAK1 and DRAK2 (Fig.2) [13, 14]. DAPK1, was the first identified member of the DAPK family, is an essential factor in interferon (IFN) γ-induced apoptosis [10]. In addition to IFN γ, the DAPK family is a group of highly related serine/threonine kinases that are associated with a wide spectrum of PCD signals such as tumor necrosis factor (TNF)-α and anoikis [13, 14]. Overexpression of the family induces apoptosis in many cancer cell lines such as HeLa cells [10, 15]. Moreover, expression of the family in cancer cells significantly decreases by methylation of its promoters [13, 16]. Thus, the DAPK family is regarded as tumor suppressor gene. Overexpression of the family causes membrane blebbing via phosphorylation of myosin light chain-2 (MLC2), resulting in apoptosis induction [17]. But, other mechanisms and regulations of apoptosis by the family are not clear.

DAPK1 is well studied in the DAPK family. In addition to apoptosis, DAPK1 associates cell adhesion [18] and autophagy [19]. DAPK1 has many domains compared with other members. The kinase contains kinase domain, Ca^{2+}/Calmodulin(CaM)-binding domain, ankyrin repeats, Ras of complex(ROC)-C-terminal of ROC(COR) domain, death domain and Ser rith tail (Fig.2) [14]. DAPK1 was reported to bind to several oncogene and cancer suppresser gene products [20]. For example, DAPK1 phosphorylates oncogene peptidyl-prolyl isomerase, protein NIMA-interacting 1 (Pin1) and inhibits activity of the protein [21]. Oncogene Src phosphorylates DAPK1 and inhibits DAPK1 activity [22]. Moreover, DAPK1 is activated by p38 that respond to ER stress [23]. DAPK1 phosphorylates and activates p53 (Fig.3) [24, 25].

The DAPK family has high sequence homology in kinase domain whereas C-terminal regulatory domains are difficult from each other (Fig.2) [13, 14]. DAPK1 binds actin filaments and localizes in cytoskeleton. From this, DAPK1 is showed to associate especially anoikis (apoptosis due to loss of cell adhesion) in apoptosis. DAPK1 suppresses cell adhesion factor integrin, and results in anoikis [26]. On the other hand, DAPK3 localized in nuclear [14, 27, 28] and associates transcriptional regulation [28]. For example, DAPK3 activates transcription factor signal transducer and activator of transcription 3 (STAT3) by phosphorylation [29].

DAPK2 has Ca^{2+}/CaM-binding domain that shows high sequence homology with DAPK1 [13,14]. DAPK2 is suggested to play a role in autophagy and anoikis, like DAPK1. Function of DAPK2 remains to be clarified. Recently, 14-3-3 protein was identified as an interaction partner of DAPK2 [15] and raptor was identified as a substrate (Fig.3) [30].

In this study, DAPK2 was identified as a substrate of cGMP-dependent protein kinase I, and β-tubulin was identified as an interaction partner of DAPK2.

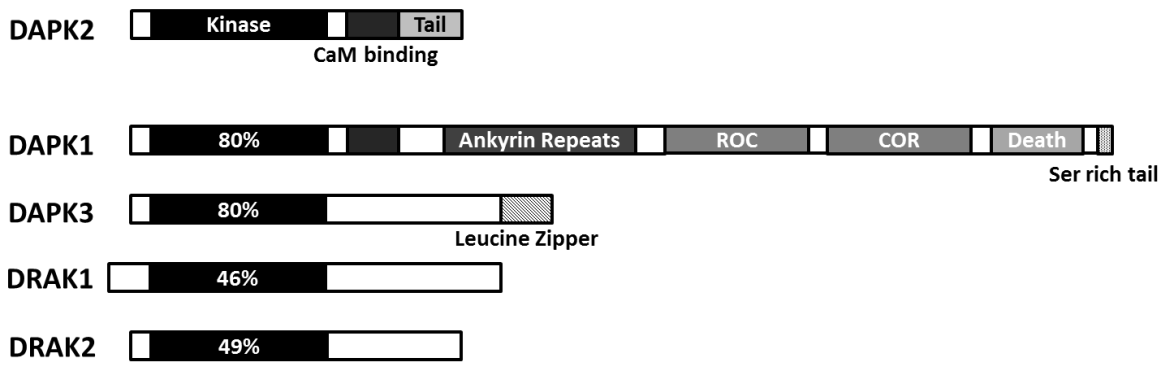

Fig.2 Domain structure of the DAPK family

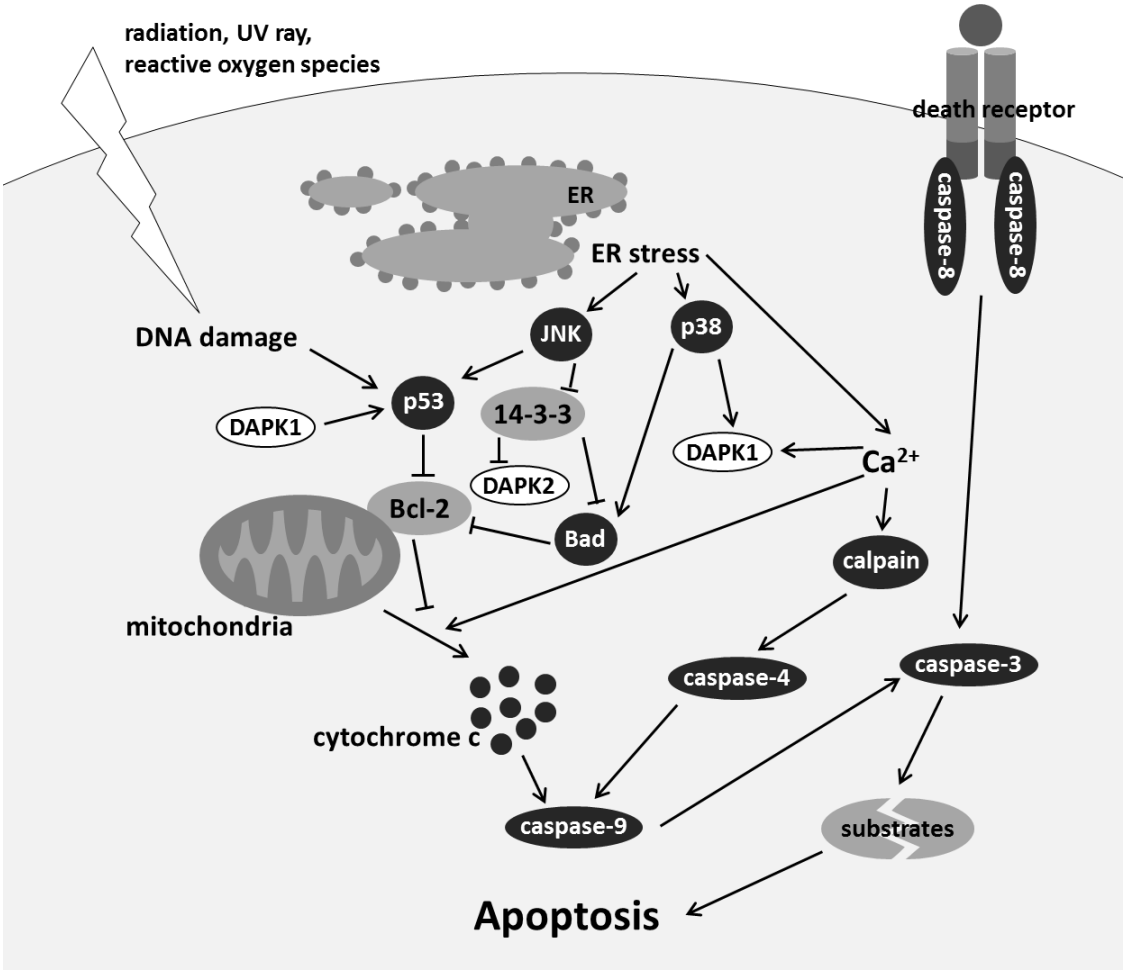

Fig.3 DAPK family and apoptosis signaling

1.4. cGMP-dependent protein kinase I (cGK-I)

cGMP-dependent protein kinase is activated by the intracellular second messenger cGMP. cGMP is generated by guanylate cyclases in response to natriuretic peptides and nitric oxide (NO). Two genes encoding for cGK-I and cGK-II have been identified, of which cGK-I has two splicing isoforms: cGK-Iα and cGK-Iß [31]. cGMP/cGK signaling has many physiological functions including smooth muscle relaxation. Recently, the signaling has been shown to be associated with anti-tumor activities, including induction of apoptosis and inhibition of metastasis and angiogenesis in many cell types (Fig.4) [32–34]. Treatment of human breast cancer cell lines, MCF-7 and MDA-MB-468, with a cell-membrane permeable cGMP analog resulted in cell growth inhibition and apoptosis induction [35, 36]. On the other hand, the expression of cGK-I isoforms is reduced in many tumors compared to normal tissues, and ectopic expression of cGK-Iß results in decreased tumor growth and invasiveness in nude mouse xenografts [36]. In addition, ectopic expression of cGK-I isoforms in the human colon carcinoma lines SW480 and SW620, which do not express endogenous cGK-I, promoted anoikis [37]. A pro-apoptotic drug exisulind, an inhibitor of cGMP phosphodiesterase PDE5, increased intracellular cGMP levels in SW480 cells [38]. Furthermore, exisulind treatment resulted in induction of cGK-Iß protein expression in addition to enzyme activation. Thus, it is highly likely that cGK activation is correlated with tumor cell apoptosis. Although recent studies suggested the involvement of the oncogene ß-catenin and c-jun N-terminal kinase in cGMP/cGK-induced apoptosis [39–41], the detailed mechanism remains unknown.

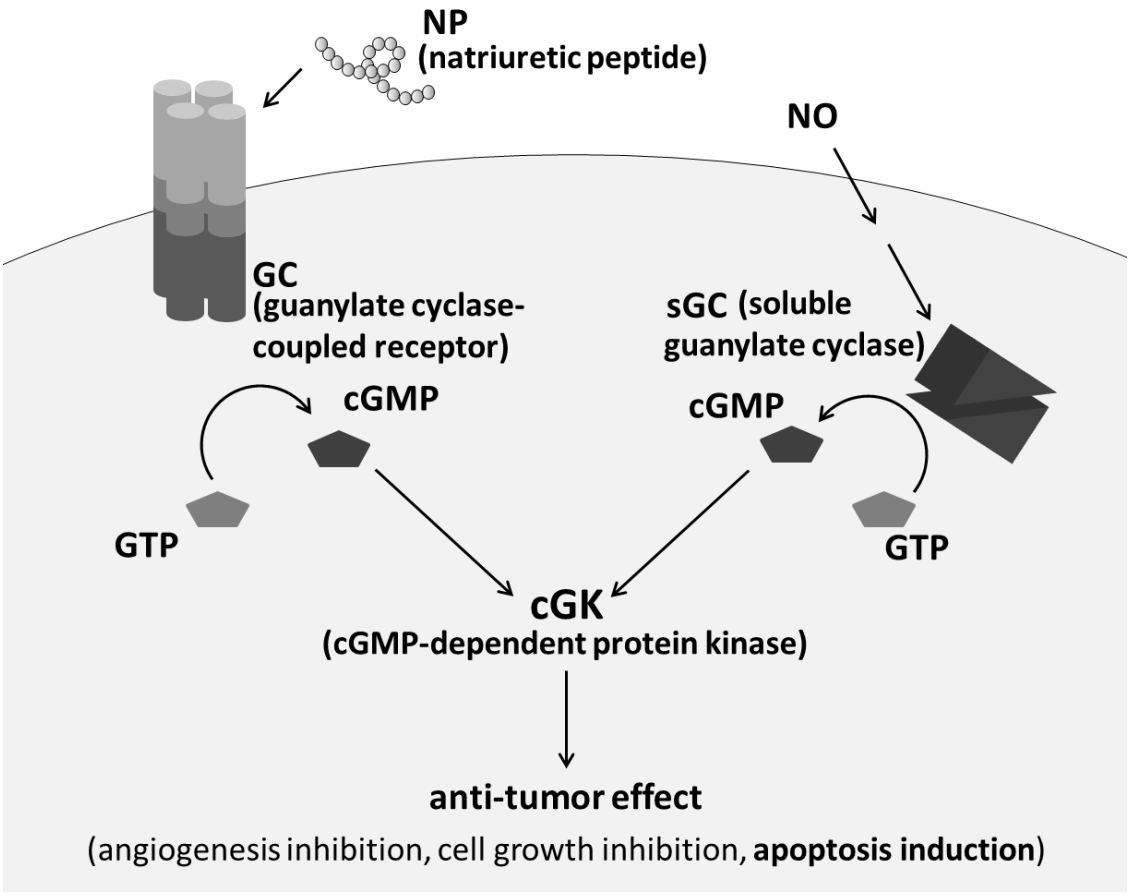

Fig.4 cGMP/cGK signaling

1.5. Tubulin and microtubule

Microtubules, which are composed of α/ß tubulin heterodimers, are a major component of the cytoskeleton. Microtubule dynamics (polymerization and depolymerization) are regulated by the coordinated action of microtubule-stabilizing (eg, XMAP-215) [42] and microtubule-destabilizing factors including microtubule depolymerizing factor (eg, kinesin-13) [43] and tubulin sequestering factor (eg, stathmin) [44]. Microtubule plays a pivotal role not only in cell migration and polarization but also in mitosis and the cell cycle, especially the formation of the spindle apparatus.

Antimicrotubule agents including polymerizing (eg, paclitaxel) and depolymerizing (eg, vinca alkaloid and nocodazole) agents interfere with these dynamic processes, resulting in apoptotic cell death. Therefore, several antimicrotubule agents are used as anticancer drugs [45]. Nocodazole is a well-known inhibitor of microtubule polymerization and arrests cell-cycle at the G2/M phase. Disruption of microtubules with nocodazole has been known to influence signal transduction events: for example, disruption of the complex between Smads and microtubules [46], and tubulin phosphorylation by cyclin-dependent kinase 1 [47].

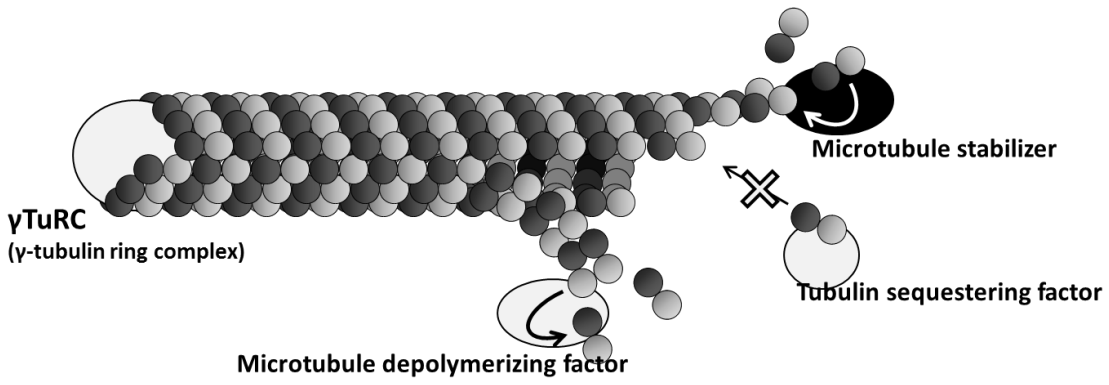

Fig.5 Regulation of microtubule

Chapter 2. Mechanism of DAPK2 regulation

2.1. Introduction

cGK has an anti-tumor activity such as induction of apoptosis and inhibition of angiogenesis [32-34]. But, especially, mechanism for induction of apoptosis by cGK is not fully understood. In this study, DAPK2 was identified as a novel substrate for cGK-I using a protein microarray. cGK-I phosphorylated DAPK2 at Ser^{299}, Ser^{367} and Ser^{368}. Phosphorylation of DAPK2 at Ser^{299} enhanced its kinase activity. Furthermore, overexpression of a phospho-mimic DAPK2 mutant, DAPK2 S299D, strongly induced apoptosis in human breast cancer MCF-7 cells compared with wild-type DAPK2. These findings highlight the importance of the cGK-I/DAPK2 signaling pathway in regulating apoptosis.

2.2. Materials and methods

2.2.1. Plasmid construction

cDNAs encoding mouse myosin light chain 2 (MLC2) and mouse DAPK2 were cloned by PCR using the respective specific primers. PCR products were cloned into TA-cloning vector pGEM-T Easy (Promega), and the inserted DNA sequences were confirmed by DNA sequencing. A cDNA encoding for mouse DAPK2 was subcloned into the mammalian expression vector pFLAG-CMV-2 (Sigma). A cDNA encoding for mouse MLC2 was subcloned into a glutathione S-transferase (GST) expression vector, pGEX (GE Healthcare). Site-directed mutagenesis was performed using PrimeSTAR Mutagenesis Basal Kit (Takara Bio) according to the manufacturer's instructions. The mutation was confirmed by DNA sequencing analysis. The

sequences of primers that were used are DAPK2 S: gcggccgcggtccaggcctcgatgagg, DAPK2 As: gtcgacttaggaggtactgctcctcc, MLC2 S: ggcaagctttcgagcaagagagccaaggcc, MLC2 As: agcttagtcgtccttgtccttggcgccgtc, DAPK2 K52A S: tatgcagctgcgttcattaagaagaggcag, DAPK2 K52A As: aatgaacgcagctgcatactccagccccgt, DAPK2 S299A S: agagaggccgtggtcaacctggagaat, DAPK2 S299A As: gaccacggcctctctgcgtaccatagc, DAPK2 S299D S: agagaggacgtcgtcaacctggagaat, DAPK2 S299D As: gacgacctcctctctgcgtaccatagt, DAPK2 S318A S: aagctagctttcagcatcgtctccttg, DAPK2 S318A As: gctgaaagctagcttccaccgcctgcg, DAPK2 S318E S: aagctcgagttcagcatcgtctccttg, DAPK2 S318E As: gctgaactcgagcttccaccgcctgcg, DAPK2 S367Δ S: aggaggtgaagtacctcctaagtcgac, DAPK2 S367Δ As: ggtacttcacctcctccgggggtgaag, DAPK2 S367D/S368D As: ttaggtgtcatccctcctccgggggtc and DAPK2 S367D/S368D/T369T As: ttaatcgtcatccctcctccgggggtg.

2.2.2. Cell culture and transfection

COS-7 and MCF-7 cells were cultured in Dulbecco's modified Eagle's medium supplemented with 10% fetal bovine serum, 100 units/ml penicillin and 100 μg/ml streptomycin at 37 ºC in 5% CO_2. Transfection was performed using Lipofectamine 2000 (Invitrogen), according to the manufacturer's instructions.

2.2.3. Protein microarray

ProtoArray Human Protein Microarray Kinase Substrate Identification (KSI) Complete Kit (Invitrogen) was used according to the manufacturer's instructions. After equilibration at 4 ºC for 15 min, the arrays were blocked with 1% bovine

serum albumin in phosphate-buffered saline (PBS) for 2 h at 4 ºC. 120 µl of kinase buffer [100 mM MOPS, pH 7.2, 1% Nonidet P40, 100 mM NaCl, 10 mg/ml BSA, 5 mM $MgCl_2$, 5 mM $MnCl_2$, 1 mM dithiothreitol and 10 µCi/µl of [γ-^{33}P]ATP (33 nM final concentration) (Perkin Elmer)] containing 50 nM purified bovine cGK-Ia (Promega) and 5 µM cGMP was overlaid onto the array and incubated for 1 h at 30 ºC. As a negative control, buffer was overlaid onto the array. The arrays were washed twice with 0.5% SDS and twice with H_2O at room temperature, dried and exposed to X-ray films. Radio-active spots were identified using GenePix Pro (Molecular Devices).

2.2.4. In vitro kinase assay

In vitro phosphorylation by cGK-I was performed as previously described [48]. MLC2 was used as a substrate for a DAPK2 activity assay. GST–MLC2 fusion protein was expressed in Escherichia coli and purified as previously described [48]. COS-7 cells transfected with pFLAG-DAPK2 wild type or mutant, were harvested with TNE buffer (20 mM Tris–HCl pH 7.5, 150 mM NaCl, 1% NP-40 and 1 mM EDTA) supplemented with protease inhibitors (10 µg/ml leupeptin and 10 µg/ml aprotinin). Cell lysates were incubated with an anti-FLAG M2 antibody (Sigma) and protein G Sepharose (GE Healthcare) overnight at 4 ºC. The beads were washed three times with TNE buffer and twice with 50 mM Tris–HCl, pH7.5. The kinase reaction was carried out by resuspending the complexes in 100 µl of kinase buffer [50 mM Tris–HCl pH 7.5, 20 mM magnesium acetate, 100 µM or 50 µM ATP, 2 µCi [γ-^{32}P]ATP, phosphatase inhibitor cocktail (Nacalai Tesque) and 30 µg/ml purified GST–MLC2] including either 100 mM $CaCl_2$ and 10 nM CaM, or 5 mM EGTA, and

incubated for 30 min at 30 ºC. Phosphorylated GST–MLC2 was separated by SDS–PAGE and visualized with a BAS-1500 Bioimaging Analyzer (Fuji Film). Quantitative densitometric analysis was performed using Image J.

2.2.5. Analysis of apoptosis

MCF-7 cells were co-transiently transfected with either FLAG-tagged DAPK2 wild type or mutants and a green fluorescent protein (GFP) plasmid. Twenty-four hours after transfection, cells were stained with Hoechst 33342 (Invitrogen) for 10 min at 37 ºC in 5% CO_2. Cells were washed with PBS and fixed with 3.7% formaldehyde in PBS for 30 min at room temperature. After washing with PBS, GFP-expressing cells were observed with a fluorescence microscope (IX71, Olympus). The number of apoptotic cells displaying both membrane blebbing and nuclear condensation was counted and expressed as a percentage of the total cell number; a minimum of 50 randomly chosen cells were counted for each sample.

2.3. Results

2.3.1. Identification of putative substrates for cGK-I by protein microarray analysis

To identify novel cGK substrates implicated in inducing apoptosis, a human protein microarray spotted with 1700 GST-tagged proteins in duplicate was used. The microarrays were incubated with [γ-^{33}P]ATP in the presence or absence of cGMP/cGK-Ia. Spots A1–4 and J13–14 on both arrays were protein kinases that were autophosphorylated in the presence of ATP (Fig. 6). Some spots with strong signals were found on the array incubated with cGMP and cGK-Iα (Fig. 6B) as compared with the control array (Fig. 6A). Spots F11–12, which were spotted with

GST–DAPK2, showed greater than 20-fold differences in their signal intensities. DAPK2 is a Ca^{2+}/CaM-dependent protein kinase belonging to the DAPK family [11]. This family consists of five members and acts as a positive regulator of apoptosis [11–13, 49, 50]. Human DAPK2 possessed three potential phosphorylation sites, $RRES^{299}$, $RRRS^{367}$ and $RRSS^{368}$ for cGK (RR/KXS/T). These sequences are also conserved in mouse and rat DAPK2. These results suggest that DAPK2 is a putative substrate for cGK-I.

Amino acid sequence analysis of human DAPK1 indicated that DAPK1 also has some potential phosphorylation sites for cGK, suggesting that DAPK1 is also phosphorylated by cGK. However, the author missed to identify DAPK1 as a novel substrate for cGK-I using protein microarray, because only small amount of GST–DAPK1 protein (nearly one-tenth of GST–DAPK2 protein) was spotted (data not shown).

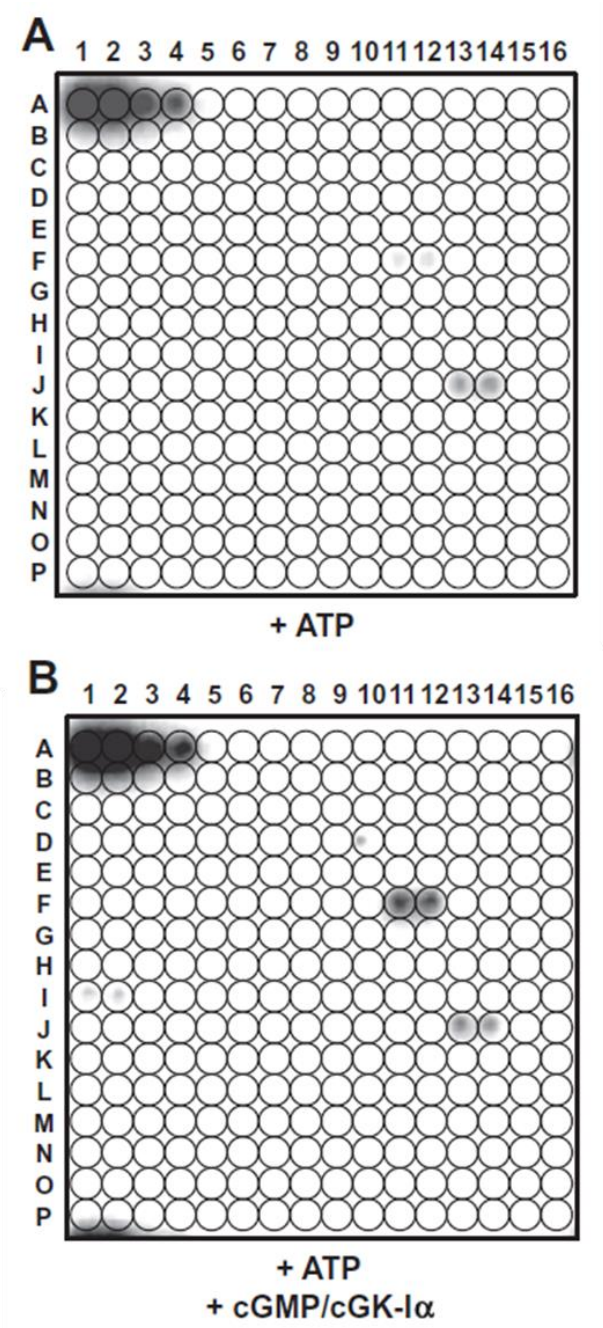

Fig. 6. Identification of DAPK2 as a putative substrate for cGK-I by protein microarray analysis. Human protein microarrays were incubated with [γ-^{33}P]ATP in the absence (A) or presence (B) of cGMP/cGK-Iα. After 30 min, the arrays were dried and exposed to X-ray films. At positions A1-4 and J13-14, protein kinases were autophosphorylated in the presence of ATP. Positions F11-12 were spotted with GST-DAPK2.

2.3.2. cGK-Ib phosphorylates DAPK2 at Ser^{299}, Ser^{367} and Ser^{368}

To confirm the protein microarray results, phosphorylation of DAPK2 by cGK in an *in vitro* kinase assay was analyzed. COS-7 cells were transfected with FLAG-tagged mouse DAPK2 along with FLAG-tagged cGK-Iß. Cell lysates were immunoprecipitated with an anti-FLAG antibody, and the immunocomplex was incubated with [γ-^{32}P]ATP in the presence or absence of cGMP. As shown in Fig. 7A, wild-type DAPK2 was phosphorylated even without cGMP and cGK-Iß. These results indicated that DAPK2 was autophosphorylated as reported previously [11, 50]. To detect cGMP/cGK-mediated phosphorylation of DAPK2, the author produced a kinase-dead mutant, DAPK2 K52A, and assessed it with an in vitro kinase assay. DAPK2 K52A was not autophosphorylated, but was efficiently phosphorylated by cGK-Iß in a cGMP-dependent manner (Fig. 7A). These data confirmed that DAPK2 was phosphorylated by cGK-I in vitro.

DAPK2 has three potential sites for phosphorylation by cGK: Ser^{299}, Ser^{367} and Ser^{368}. To identify DAPK2 sites phosphorylated by cGK-I, the author created phospho-resistant mutants for these sites. Ser^{299} was replaced by non-phosphorylatable Ala (DAPK2 K52A/S299A). Because DAPK2 is a protein comprised of 370 amino acids and its Ser^{367} and Ser^{368} residues are close to the C-terminal end, Ser^{367} was replaced by a stop codon, DAPK2 K52A/367Δ. As shown in Fig. 7B, an *in vitro* kinase assay demonstrated that the phosphorylation of both DAPK2 K52A/S299A and K52A/367Δ by cGK-Iß were reduced compared with that of DAPK2 K52A. Furthermore, cGK-Iß failed to phosphorylate a triple mutant, DAPK2 K52A/S299A/367Δ. These results suggest that cGK-I phosphorylates DAPK2 at Ser^{299}, Ser^{367} and Ser^{368}.

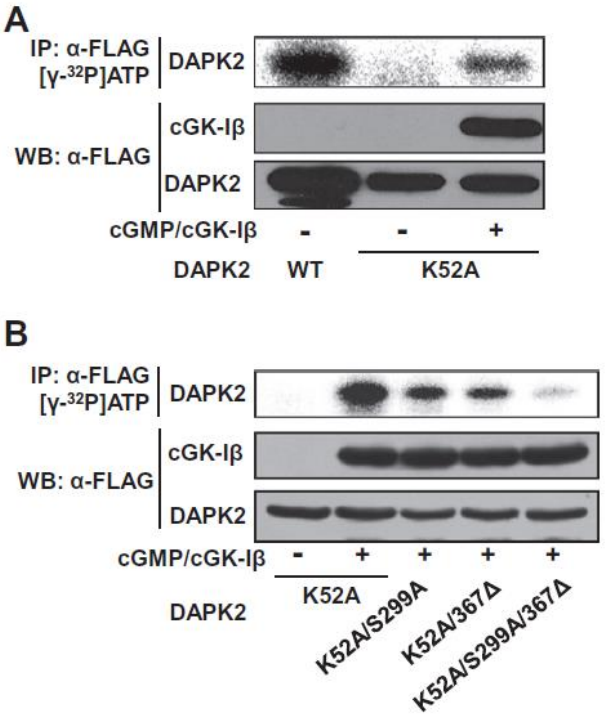

Fig. 7. cGK-I phosphorylates DAPK2 at Ser^{299}, Ser^{367} and Ser^{368}. (A and B) FLAG-tagged DAPK2 wild type or mutant was expressed in COS-7 cells along with FLAG-tagged cGK-Iß. FLAG-tagged proteins were immunoprecipitated and incubated in a kinase buffer containing [γ-^{32}P]ATP with or without cGMP. To monitor the expression level of the FLAG-tagged proteins, cell lysates were blotted with an anti-FLAG antibody.

2.3.3. Phosphorylation of DAPK2 at Ser^{299} by cGK-I increases its kinase activity

Next, affect of DAPK2 phosphorylation on its kinase activity was studied. Three putative phosphorylation sequences (RRES^{299}, RRRS^{367} and RRSS^{368}) were completely matched to the consensus motif for cGK (RR/KXS/T), RSST^{369} also partially corresponded to this phosphorylation motif. Thus, three phospho-mimic mutants were generated in which the putative cGK phosphorylation sites were replaced by Asp: DAPK2 S299D, DAPK2 S367D/S368D and DAPK2 S367D/S368D/T369D. MLC2 was used as a substrate for DAPK activity as previously described [13]. As shown in Fig. 8A, wild-type DAPK2 phosphorylated GST–MLC2 in a Ca^{2+}/CaM-dependent manner (3.4-fold increase). Interestingly, the activity of the DAPK2 S299D mutant was significantly increased (two fold increase) compared with that of the wild type in the presence of Ca^{2+}/CaM, whereas the activities of DAPK2 S367D/S368D and DAPK2 S367D/S368D/T369D mutants were

not changed. In addition, the DAPK2 S299D mutant showed a significantly high activity even without Ca^{2+}/CaM. The activity of another phospho-mimic mutant, DAPK2 S299E, was also examined. As expected, the DAPK2 S299E mutant also exhibited enhanced kinase activity like that of the DAPK2 S299D mutant (Fig. 8B). These findings suggested that phosphorylation of DAPK2 at Ser^{299}, but not at Ser^{367} and Ser^{368}, stimulated its kinase activity independently of Ca^{2+}/CaM.

A previous study demonstrated that DAPK2 was inactivated by autophosphorylated at Ser^{318}, and that DAPK2 activation is required for dephosphorylation of Ser^{318} [51]. To examine whether phosphorylation of Ser^{299} affects autoinhibition by phosphorylation at Ser^{318}, DAPK2 S318E and DAPK2 S299D/ S318E mutants were created and these kinase activity were examined by *in vitro* kinase assay. As shown in Fig. 8C, the DAPK2 S318E mutant was not activated by Ca^{2+}/CaM, consistent with a previous report [51]. On the other hand, the kinase activity of the DAPK2 S299D/S318E double mutant was similar to that of the DAPK2 S299D mutant and overcame the inhibitory effect of phosphorylation at Ser^{318}. These results suggested that DAPK2 phosphorylation at Ser^{299} increased its kinase activity by a Ca^{2+}/CaM-independent mechanism and also interfered with the autoinhibitory mechanism resulting from phosphorylation at Ser^{318}.

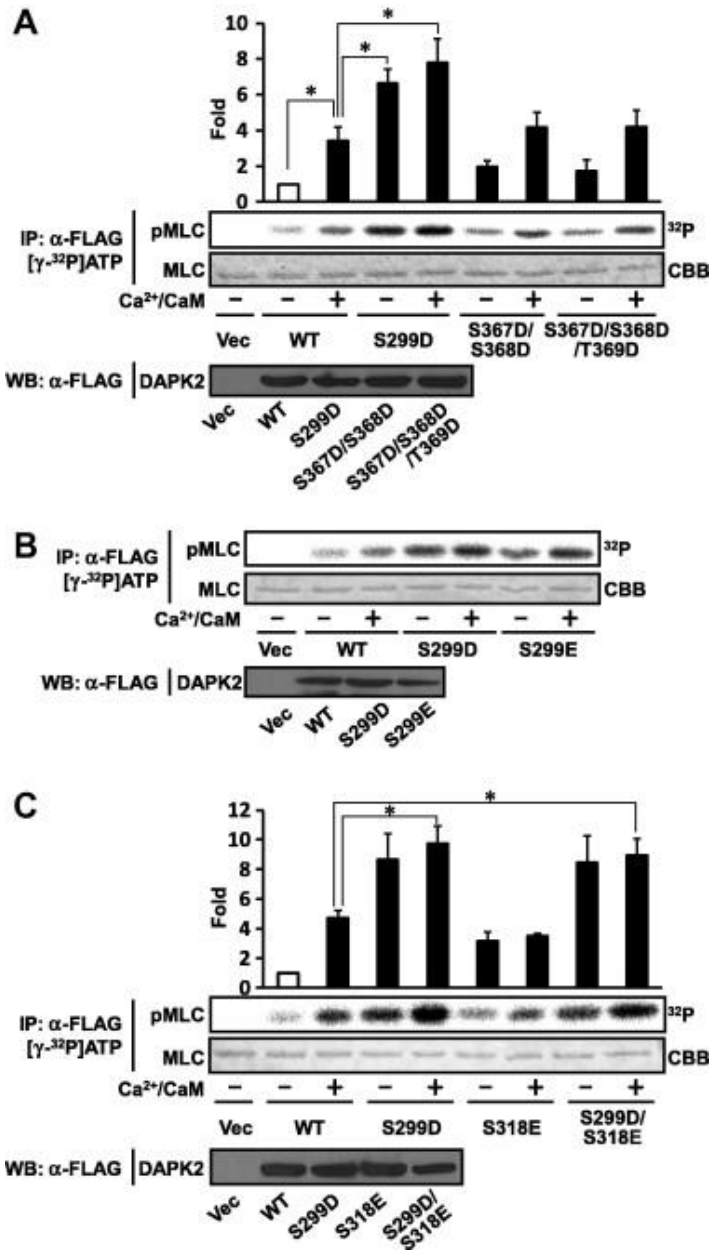

Fig. 8. Phosphorylation of DAPK2 at Ser^{299} enhances its kinase activity. (A, B and C) COS-7 cells were transiently transfected with FLAG-DAPK2 wild type or mutant. FLAG-DAPK2 proteins were immunoprecipitated and used in an in vitro kinase assay with recombinant GST-MLC2 as a substrate in the presence of either $CaCl_2$/CaM or EGTA. GST-MLC2 was separated on SDS-PAGE, after which the gel was analyzed by Coomassie blue staining and a bioimaging analyzer. The relative kinase activity of DAPK2 was quantified by densitometric analysis. The activity of wildtype DAPK2 without Ca^{2+}/CaM was taken as 1. All experiments were performed three times independently. Results are expressed as means ± S.E. Statistical significance was determined by Student's t-test. *$P < 0.05$, **$P < 0.01$.

2.3.4. A phospho-mimic mutant DAPK2 S299D strongly induces apoptosis compared with wild-type DAPK2

A previous study showed that DAPK2 overexpression induced apoptosis in various cell lines, and that a dominant-negative DAPK2 mutant protected cells from TNF-α-induced apoptosis [11]. These results suggested a strong association between DAPK2 catalytic activity and apoptosis. In order to know role of DAPK2 in apoptosis precisely, relationship effect of DAPK2 phosphorylation at Ser^{299} the induction of apoptosis were investigated on human breast cancer MCF-7 cells. In a previous study [17], apoptotic morphological changes, such as membrane blebbing and nuclear condensation, were clearly observed in MCF-7 cells that were transfected with DAPK2. MCF-7 cells were transiently transfected either DAPK2 wild type or mutants along with GFP. In GFP-expressing cells, the number of apoptotic cells displaying both membrane blebbing and nuclear condensation was counted. As shown in Fig. 9, overexpression of wild-type DAPK2 significantly induced apoptosis, whereas a DAPK2 inactive mutant, S318E, induced fewer apoptotic changes than wild type consistent with a previous report [51]. In agreement with the data for kinase activity, forced expression of the phospho-mimic mutant DAPK2 S299D resulted in a two fold increase in apoptotic cells compared with wild-type DAPK2. In addition, the same result was observed for DAPK2 S299D/S318E-expresseing cells. These results suggested that cGK-I induced apoptosis through DAPK2 phosphorylation.

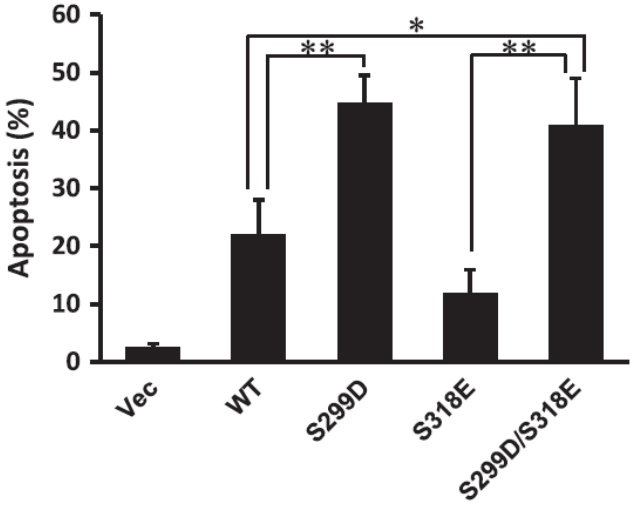

Fig. 9. Phospho-mimic mutant DAPK2 S299D enhances apoptosis induction in MCF-7 cells. pFLAG-DAPK2 wild type or mutant was transiently transfected into MCF-7 cells along with pEGFP. After 24 h, cells were stained with Hoechst 33342 and fixed with formaldehyde. Fixed cells were observed under a fluorescence microscope. The number of cells showing apoptotic morphologies was expressed as a percentage of the total number of GFP-expressing cells counted. Experiments were performed three times independently. Results are expressed as means ± S.E. Statistical significance was determined by Student's t-test. *$P < 0.05$, **$P < 0.01$.

2.4. Discussion

cGMP/cGK signaling can induce apoptosis in cancer cell lines and it has been suggested that this signaling pathway could be a target for anti-cancer agents [32–34]. However, the detailed signaling mechanisms remain unclear. In this study, the author identified DAPK2 as a novel cGK substrate using protein microarray technology. DAPK2 belongs to the DAPK family comprised of five kinases that share a high sequence homology in their catalytic domains and are involved in apoptosis induction. DAPK2 is a CaM-dependent serine/threonine kinase that is activated by CaM in response to Ca^{2+} stimuli. In addition to its activation by Ca^{2+}/CaM, DAPK2

activity is also regulated by an autoinhibitory mechanism. By the mechanism called a “double-locking” mechanism, DAPK2 is kept in an inactive state [51]. DAPK2 activation is required for dephosphorylation of an autophosphorylated residue Ser^{318} within the CaM-binding domain. The negative charge of its phospho-Ser^{318} residue interacts with the positive charge of a Lys^{151} residue in its active site, which results in the inhibition of CaM binding. This autoinhibitory mechanism is necessary to prevent erroneous activation in response to random fluctuations in cellular Ca^{2+} levels. The author found that DAPK2 phosphorylation at Ser^{299} increased its kinase activity in a Ca^{2+}/CaM-independent manner and overcame the autoinhibitory mechanism resulting from phosphorylation at Ser^{318}. Because the Ser^{299} residue phosphorylated by cGK-I is also located in the CaM-binding domain and is close to the autophosphorylation Ser^{318} site, the author suggests that DAPK2 phosphorylation at Ser^{299} could disrupt the interaction between phospho-Ser^{318} and Lys^{151} and promote Ca^{2+}/CaM binding, thus triggering DAPK2 hyperactivation. However, a CaM overlay assay revealed that a phospho-mimic mutation at Ser^{299} did not influence the binding of CaM to DAPK2 (data not shown). DAPK2 activity has also been shown to be regulated by dimerization [51, 52]. This suggests that other mechanisms may be involved in the hyperactivation of DAPK2 by Ser^{299} phosphorylation. DAPK1 and DAPK2 show high sequence homology in their CaM binding domains and have conserved autophosphorylation sites [51, 53]. Sequence alignments indicate that DAPK1 has a Ser^{289} residue corresponding to Ser^{299} in DAPK2. Interestingly, a previous study showed that DAPK1 phosphorylation at Ser^{289} by p90 ribosomal S6 kinase inhibited its pro-apoptotic activity in a non-tumor cell line, HEK293E [54]. However, my findings may be supported by another study

that showed that DAPK2 was activated via transphosphorylation of residue(s) other than Ser^{318} by unidentified kinase(s) [51]. Because the autoinhibitory mechanism of DAPK2 has been shown to be different from that of DAPK1 [52], phosphorylation at Ser^{289} in DAPK1 and Ser^{299} in DAPK2 may exert opposite effects.

In cancer cell lines, the expression of DAPK2 is generally silenced by hypermethylation of its promoter [13]. However, a previous report showed that knockdown of oncogenic β-catenin by RNA interference induced DAPK2 expression in a colon cancer cell line [55]. This cell line lacked a functional adenomatous polyposis coli (APC) tumor suppressor protein. Although APC induces β-catenin degradation in normal cells, which is dependent on phosphorylation by glycogen synthase kinase 3β, its degradation is often blocked by loss-of-function mutations of APC in carcinomas. On the other hand, cGMP/cGK signaling attenuates β-catenin-mediated transcription but not β-catenin degradation in colon and breast cancer cells, although the downstream target(s) directly regulated by cGK remain unclear [39, 41]. Taken together, cGMP/cGK-I signaling may increase DAPK2 expression via suppression of β-catenin-mediated transcription and activate DAPK2 via phosphorylation at Ser^{299}, resulting in induction of apoptosis in cancer cells.

In summary, DAPK2 was identified a novel cGK-I substrate implicated in apoptosis induction. DAPK2 kinase activity was regulated by its trans-phosphorylation. Phosphorylation of DAPK2 at Ser^{299} enhanced its kinase activity, which resulted in inducing apoptosis in MCF-7 cells.

Chapter 3. Mechanism of apoptosis induction

3.1. Introduction

In this study, I identified ß-tubulin as a novel DAPK2-interacting partner using a pull-down and mass spectrometry approach.

During nocodazole-induced apoptosis, DAPK2 strongly interacted with tubulin. Furthermore, the author found that DAPK2 knockdown resulted in a significant suppression of nocodazole-induced apoptotic cell death. These findings showed that DAPK2 mediates nocodazole-induced apoptosis through interaction with tubulin.

3.2. Materials and methods

3.2.1. Antibodies

Antibody against DAPK2 was purchased from Millipore. Anti-FLAG M2 antibody was from Sigma. Anti-Strep antibody was purchased from Qiagen. Anti-α-tubulin and anti-pan-14-3-3 antibodies were from Santa Cruz Biotechnology. Anti-PARP antibody was purchased from Cell Signaling Technology. Anti-GST antibody was purchased from Wako Pure Chemical Industries.

3.2.2. Plasmid construction

The expression plasmids pFLAG-DAPK2 and p105-DAPK2 encoding mouse DAPK2 was described previously [15, 56]. cDNAs encoding human ß-tubulin were cloned by PCR using the respective specific primers. PCR products were cloned into TA-cloning vector pGEM-T Easy (Promega), and the inserted DNA sequences were confirmed by DNA sequencing. cDNA encodings for mouse DAPK2 and ß-tubulin

were subcloned into the mammalian expression vector pFLAG-CMV-2 (Sigma), pEBG and pEXPR-IBA105 (IBA). Site-directed mutagenesis and deletion mutagenesis were performed using PrimeSTAR Mutagenesis Basal Kit (TaKaRa Bio) according to the manufacturer's instructions. The mutation was confirmed by DNA sequencing analysis. The sequences of primers that were used are DAPK2 CD S: cacgccgtagggatccgtggacacccagcaagcta, DAPK2 CD As: tgtccacggatccctacggcgtgatccagggatgt, DAPK2 ΔCD S: cacgccgaagcttgtggacacccagcaagctat, DAPK2 ΔCD As: tgtccacaagcttcggcgtgatccagggatgtc, ß-tubulin S: ccgcggtcagggaaatcgtgcacttg and ß-tubulin As: tctagactaggccacctcctcctcagcctc.

3.2.3. Cell culture, transfection and RNA interference

HeLa and HEK293T cells were cultured in Dulbecco's modified Eagle's medium supplemented with 10% fetal bovine serum, 100 units/ml penicillin and 100 μg/ml streptomycin at 37 ºC in 5% CO_2. Transfection and RNA interference was performed using Lipofectamine 2000 (Invitrogen), according to the manufacturer's instructions. The synthetic small interfering RNA (siRNA) oligonucleotide for DAPK2 was purchased from Sigma (ID# SASI_Hs01_00206405). A MISSION siRNA Universal Negative Control #1 (Sigma) was used as the negative control. The target sequences of DAPK2 siRNA is cgccggaatttgttgctccag. In the case of DAPK2 rescue experiment, cells were transfected with pFLAG-DAPK2 after 24 hours of knockdown. Nocodazole-treatment was performed after 24 hours of transfection or knockdown.

3.2.4. Protein identification by matrix-assisted laser desorption/ionization

time-of-flight mass spectrometry (MALDI-TOF MS)

HeLa cells were transfected with p105-DAPK2. After 24 hours, cells were scraped in cell lysis buffer (20 mM Tris-HCl, pH 7.5, 150 mM NaCl, 0.5% NP40, 1 mM EDTA, 10 mM leupeptin, and 10 mg/ml aprotinin). The cell extracts were centrifuged at 10,000 ×g for 10 min at 4 ºC, and the supernatants were incubated with Strep-Tactin Sepharose (IBA) over night at 4 ºC. The beads were washed with wash buffer (20 mM Tris-HCl pH 7.5, 150 mM NaCl, 0.1% NP40, and 1 mM EDTA), and the bound proteins were eluted with 6 x SDS-loading buffer. The eluates were resolved by 10% SDS-PAGE, followed by silver staining (Silver Staining MS Kit, Wako Pure Chemical Industries). Subsequent protocol has been described previously [15]. Briefly, the bands in the SDS-PAGE gel were cut off and destained by de-staing solution (Wako Pure Chemical). The gels were dehydrated by 100% acetonitrile and were dried using a centrifugal evaporator. After this, the gels were reduced by reducing reagent (10 mM dithiothreitol and 25 mM ammonium bicarbonate) at 56 ºC for 45 min. After reduction, the gels were alkylated by alkylating reagent (55 mM iodoacetamide and 25 mM ammonium bicarbonate) for 30 min, After wash with 25 mM ammonium bicarbonate, the gels were dehydrated (using 25 mM ammonium bicarbonate/50% acetonitrile followed by 100% acetonitrile). Following the drying by centrifugal evaporator, trypsin digestion was performed over night at 37 ºC. Trypsin-digested peptides were extracted and desalted using C18 ZipTip (Millipore). The samples were mixed with the matrix, and then spotted on AnchorChip sample target (Bruker Daltonics). The mass spectra of peptides were acquired by MALDI-TOF MS (Autoflex Speed, Bruker Daltonics). The mass spectra were processed using FlexAnalysis 3.3 and Biotools

3.2 (Bruker Daltonics), and the generated data were analyzed using the Mascot server (Matrix Science).

3.2.5. Co-immunoprecipitation and pull-down assays

For a Strep or GST pull-down assay, HEK293T or HeLa cells were co-transfected with DAPK2s and ß-tubulin. After 24 hours, cells were scraped in lysis buffer. Cell lysates were incubated with Strep-Tactin or glutathione sepharose over night at 4 ºC. The bound proteins were analyzed by immunoblot analysis using anti-FLAG M2 antibody, anti-Strep antibody, and/or anti-GST antibody.

3.2.6. Apoptotic cell death assay

Apoptotic cell death was evaluated using Cell Death Detection ELISA (Roche) according to the manufacturer's instructions. After 24 hours of nocodazole treatment, cells were harvested with incubation buffer. After centrifugation, cell lysates were applied to 96 well plate coated by anti-histone antibody. Following washing, an anti-DNA antibody conjugated to peroxidase was added to each well. After washing, 2,2 -azino-bis(3-ethylbenzthiazoline)-6-sulfonic acid substrate solution for peroxidase was added to induce a colored reaction product. The absorbance of the samples was determined by using Infinite M200 plate reader (Tecan) at 405 nm.

3.3. Results

3.3.1. Identification of ß-tubulin as a novel binding partner to DAPK2.

To understand the molecular mechanisms underlying DAPK2-induced apoptosis, the author attempted to identify novel binding partners of DAPK2. The author previously identified 14-3-3 proteins as interacting proteins of DAPK2 from human breast cancer MCF-7 cells by combined Strep pull-down and MALDI-TOF MS. This approach is very useful to identify interacting proteins [15]. In this study, the Strep pull-down approach was performed using human cervix epithelial HeLa cells instead of MCF-7 cells. HeLa cells endogenously express DAPK2 protein (Fig. 11C), and a previous report has shown that overexpression of constitutively active DAPK2 in HeLa cells induces apoptosis [17]. Furthermore, HeLa cells can be transiently transfected with high efficiency and high expression levels as compared with MCF-7 cells. Threfore, HeLa cells are suggested to be suitable cells for identification of novel DAPK2-interacting proteins playing a significant role in apoptosis. After transfection into HeLa cells with Strep-tagged DAPK2, cell lysates were subjected to Strep pull-down, followed by SDS-PAGE and silver staining. As shown in Fig. 10A, the specific protein bands at 30, 31, 44, 55 and 88 kDa were found in the precipitates from cells transfected with Strep-DAPK2 as compared with those from control cells. The bands at 44 and 88 kDa are close to the molecular masses of the Strep-tagged DAPK2 and its SDS-resistant dimer, respectively. On the other hand, two bands at 30 and 31 kDa corresponding to 14-3-3 proteins were identified, consistent with the author's previous study [15]. Therefore, the 55-kDa band were excised and analyzed by MALDI-TOF MS after in-gel tryptic digestion. The analysis showed that a 55-kDa protein is ß-tubulin (Fig. 10B and 10C). To confirm the interaction between DAPK2 and ß-tubulin, the author performed a Strep pull-down experiment using lysates prepared from HEK293T cells expressing

Strep-tagged DAPK2 and FLAG-tagged ß-tubulin. As shown in Fig. 11A, Strep-DAPK2 specifically interacted with FLAG-ß-tubulin.

In the cell, most ß-tubulin forms a heterodimer with α-tubulin. Next, the author investigated the interaction between DAPK2 and α-tubulin. HEK293T cells were transfected with either Strep-DAPK2 or Strep vector. After the Strep pull-down assay, the precipitated proteins were analyzed by Western blot analysis with anti-α-tubulin antibody. As shown in Fig. 11B, Strep-DAPK2 interacted with not only ß-tubulin but also α-tubulin, indicating that DAPK2 interacts with α/ß-tubulin heterodimer. Furthermore, the author examined the endogenous interaction between DAPK2 and ß-tubulin. Endogenous expression of DAPK2 protein in HeLa cells was confirmed by knockdown analysis using siRNA (Fig. 11C). Subsequently, the author performed immunoprecipitation using the cell lysates from HeLa cells followed by Western blotting with anti-ß-tubulin antibody. When immunoprecipitated with anti-DAPK2 antibody, ß-tubulin was detected (Fig. 11C, *IP: DAPK2*). On the other hand, control IgG did not precipitate ß-tubulin (Fig. 11C, *IP: IgG*). These results support that DAPK2 and ß-tubulin are physiologically interacting partners.

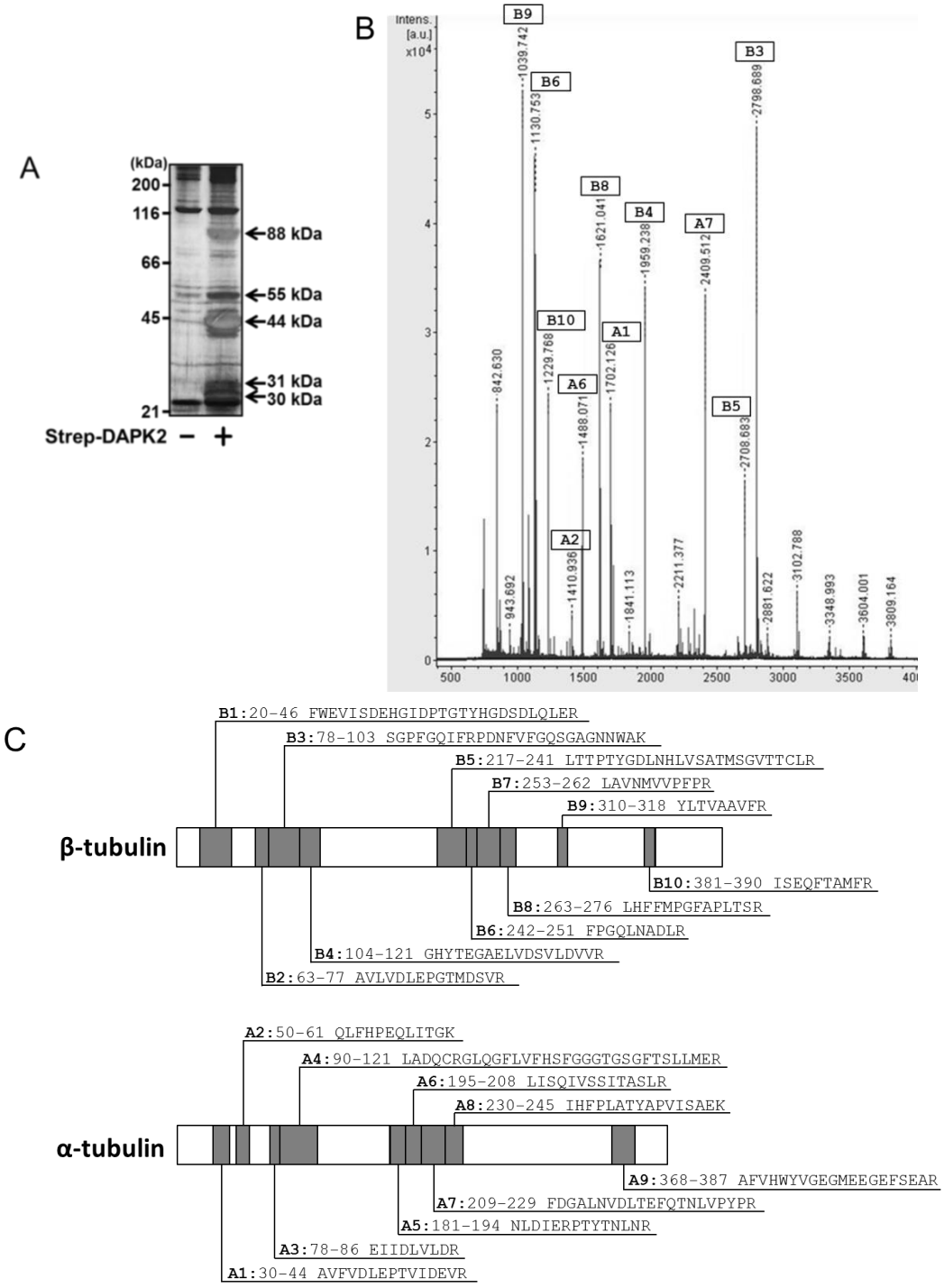

Fig. 10. Identification of β-tubulin as a binding protein for DAPK2. (A) HeLa cells were transfected with either Strep empty vector or Strep-DAPK2. After 24 hours, cells were scraped in lysis buffer and were used for Strep pull-down assay. The bound proteins were resolved by SDS-PAGE, followed by silver staining. (B)The results of MS are shown. Number of fragment is the same that is shown 10C. (C) Amino acid sequences of tubulin are shown. The gray regions were identified by MS.

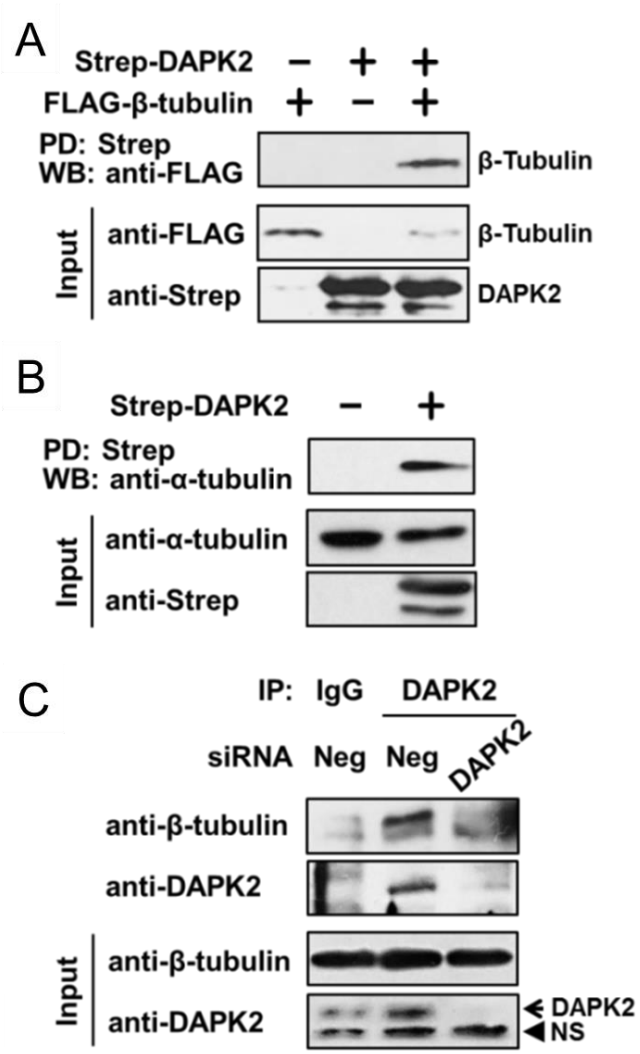

Fig11. Tubulin binds to DAPK2. (A and B) HEK293T cells were transfected with Strep-DAPK2 with or without FLAG-β-tubulin. The cell lysates were pulled down with Strep-Tactin (*PD: Strep*), followed Western blot analysis using anti-FLAG (A, *WB: anti-FLAG*) or anti-α-tubulin antibodies (B, *WB: anti-α-tubulin*). Protein expression was confirmed by Western blot analysis of total cell lysates (*Input*). (C) HeLa cells were transfected with siRNA against DAPK2 or negative control siRNA (*Neg*). The cell lysates were immunoprecipitated using either anti-DAPK2 antibody (*IP: DAPK2*) or normal rabbit IgG (*IP: IgG*). The immunoprecipitates were analyzed by Western blot analysis using anti-β-tubulin or anti-DAPK2 antibodies. The endogenous expression of β-tubulin and DAPK2 was confirmed by Western blot analysis of HeLa cell lysates with the appropriate antibodies (*Input*). *NS* indicates a nonspecific band. All experiments were performed multiple times with similar results.

3.3.2. ß-Tubulin interacts with monomeric but not dimeric DAPK2.

To identify the region of DAPK2 that interacts with ß-tubulin, interaction of deletion mutants of DAPK2; the DAPK2 catalytic domain (DAPK2 CD) and the C-terminal region lacking the catalytic domain (DAPK2 ΔCD) (Fig. 12A) with ß-tubulin were analyzed by GST pull-down assay. As shown in Fig. 12B, the author confirmed that GST-fused full-length DAPK2 (GST-DAPK2 WT) interacted with Strep-ß-tubulin. Although DAPK2 ΔCD could bind to ß-tubulin, DAPK2 CD could not, suggesting that DAPK2 interacts with ß-tubulin via its C-terminal region (amino acids 288-370). The C-terminal region of DAPK2 mediates its homodimer formation [51, 54], and additionally contains 14-3-3 binding region [15, 57]. These results suggest that the interaction between DAPK2 and ß-tubulin may influence the homodimer formation and/or 14-3-3 interaction. Thus, two FLAG-tagged DAPK2 mutants (DAPK2 Δ367 and DAPK2 T369A) were prepared. DAPK2 Δ367 mutant cannot form a homodimer and interact with 14-3-3 proteins, and DAPK2 T369A mutant shows only weak binding to 14-3-3 proteins [15]. By Strep pull-down experiments, the binding of Strep-ß-tubulin to these mutants was analyzed. Although FLAG-tagged DAPK2 wild type (FLAG-DAPK2 WT) formed a homodimer, Strep-ß-tubulin specifically interacted only with monomeric DAPK2 (Fig. 12C). On the other hand, DAPK2 Δ367 and DAPK2 T369A displayed no or little dimerization and binding to ß-tubulin. These results suggested that binding of dimeric DAPK2 to tubulin may be interfered with by its conformation and/or other binding proteins, although the C-terminus of DAPK2 is required for interaction with ß-tubulin. Additionally, although the author examined the DAPK2/ß-tubulin complex binding to 14-3-3 proteins, the interaction could not be detected, showing that 14-3-3

proteins may not be able to recognize the DAPK2/β-tubulin complex.

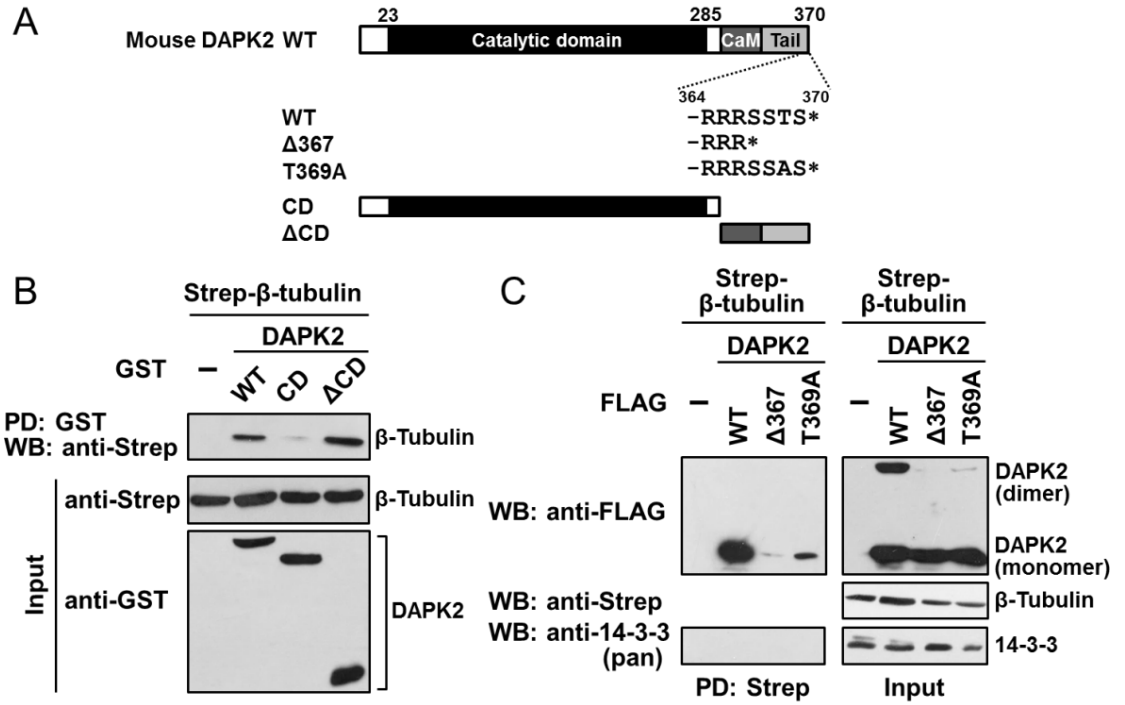

Fig. 12. β-Tubulin interacts with the C-terminal region of DAPK2. (A) Schematic representations of DAPK2 and its mutants are shown. (B) Strep-β-tubulin was co-expressed with GST-DAPK2 wild type (*WT*) or its deletion mutants (DAPK2 CD and DAPK2 ΔCD) in HEK293T cells. The cell lysates were pulled down with glutathione-Sepharose and analyzed by Western blotting using anti-Strep antibody. (C) HEK293T cells were transfected with FLAG-DAPK2 wild type (*WT*) or its mutants together with Strep-β-tubulin. Cell lysates were pulled down with Strep-Tactin (*PD: Strep*), followed Western blot analysis using anti-FLAG or anti-14-3-3 (pan) antibodies. Protein expression was confirmed by Western blot analysis of total cell lysates with the appropriate antibodies (*Input*). All experiments were performed multiple times with similar results.

3.3.3. Role of DAPK2 in nocodazole-induced apoptosis.

Because microtubule dynamics play a pivotal role in many cellular functions, their disruption results in apoptotic cell death. Nocodazole has long been used as a standard microtubule depolymerising agent, and causes apoptosis in various cells. The author investigated whether DAPK2 is involved in apoptosis induced by nocodazole. In apoptotic cells, PARP (116 kDa) is cleaved by caspases into 89- and 25-kDa fragments [58]. The author examined the level of an apoptotic marker, cleaved PARP, by Western blotting with the antibody which recognizes both the 116 kDa intact form and the 89 kDa fragment of PARP. Treatment of HeLa cells with 0.1 μg/ml nocodazole led to a 5-fold increase in ratio of cleaved PARP-to-uncleaved PARP (Fig. 13A), confirming that nocodazole induces apoptosis in HeLa cells. In DAPK2 knockdown cells, cleavage of PARP triggered by nocodazole was significantly reduced, but not completely. These results were further confirmed by using another apoptosis assay, which is determined by measuring cytoplasmic histone-associated DNA fragments (Fig. 13B), showing that DAPK2 partially mediates nocodazole-induced apoptosis. Finally, the author investigated whether DAPK2-tubulin interaction is associated with nocodazole-induced apoptosis. As shown in Fig. 14, Strep pull-down analysis using the cells treated with nocodazole revealed that DAPK2-tubulin interaction was extremely enhanced by nocodazole treatment.

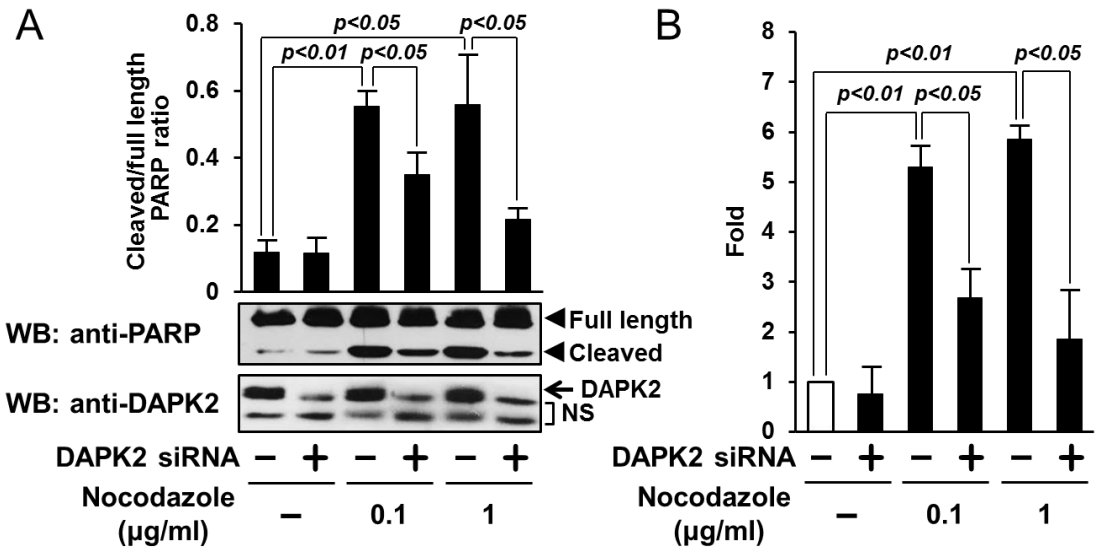

Fig. 13. DAPK2 partially mediates nocodazole-induced apoptosis. (A) HeLa cells were transfected with DAPK2 siRNA or negative control siRNA. After 24 hours transfection, cells were treated with 0.1 or 1 μg/ml nocodazole or DMSO as a control for 24 hours. Total cell lysates were subsequently analyzed by Western blot analysis using anti-PARP or anti-DAPK2 antibodies. The bands of full-length and cleaved PARP were quantitated using Image J software. The ratio of cleaved PARP/full-length PARP is showed in the graph. Results are expressed as means ± S.E. of three different experiments, and statistical significance was determined by Student's t-test. *NS* indicates a nonspecific band. (B) HeLa cells transfected with DAPK2 siRNA or negative control siRNA were exposed to DMSO (control, -) or nocodazole (0.1 and 1 μg/ml) for 24 hours. The quantitative determination of cytoplasmic histone-associated DNA fragments was conducted using a Cell Death Detection ELISA Kit. Results were expressed as fold induction relative to the values obtained from negative control siRNA-transfected cells treated with DMSO (*opened bar*). The data shown are the means ± S.E. derived three independent experiments, and statistical significance was determined by Student's t-test.

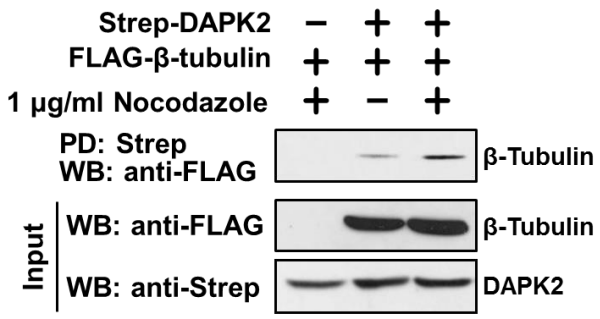

Fig. 14. Nocodazole-treatment enhanced DAPK2-β-tubulin interaction. HEK293T cells transfected with Strep-DAPK2 in combination with FLAG-β-tubulin were treated with 1 μg/ml nocodazole or DMSO as a control for 10 hours. The cell lysates were used for Strep pull-down experiments. Protein expression was confirmed by Western blot analysis using the appropriate antibodies. Similar results were obtained in two additional experiments. The experiment was performed multiple times with similar results.

3.4. Discussion

Although the DAPK family shows high homology in the N-terminal catalytic domain, the C-terminal regulatory domains are different from each other. Therefore, it is suggested that the C-terminal regions define their physiological functions via different interacting partners and/or specific subcellular localization. The C-terminal region of DAPK2 contains a CaM binding domain and a 40-amino acid C-terminal tail, which shows no homology to other DAPK family members and mediates its homodimerization. Moreover, the author's and others recent studies [15, 57] showed that 14-3-3 proteins binds to the serine/threonine-rich sequence in the C-terminal tail of DAPK2 in a phosphorylation-dependent manner and suppressed its kinase activity and subsequently apoptosis, suggesting unique regulation of DAPK2 by 14-3-3 proteins. In this study, the author identified

ß-tubulin as a novel DAPK2-interacting partner from HeLa cells, using a combined pull-down and MS approach. Only monomeric but not dimeric DAPK2 bound to α/ß-tubulin heterodimers via its unique C-terminal region. Structural analysis indicated that the monomerization of DAPK2 is necessary for enzymatic activation [54], suggesting that monomeric DAPK2 bound to tubulin is enzymatic active. Thus, the author examined the involvement of DAPK2 in microtubule disruption-induced apoptosis. Although the microtubule polymerization inhibitor nocodazole, which elevates intracellular Ca^{2+} concentration [59], induced apoptosis, siRNA-mediated silencing of the DAPK2 gene significantly suppressed the induction of apoptosis. Additionally, nocodazole promoted the formation of the DAPK2-tubulin complex. DAPK2 phosphorylated by the survival kinase Akt is associated with 14-3-3 proteins in growing cells, while Ca^{2+}/CaM-regulated protein phosphatase, calcineurin, dephosphorylates DAPK2, resulting in dissociation from 14-3-3 proteins [15]. Taken together, monomeric DAPK2 released from 14-3-3 proteins by nocodazole treatment, may bind to α/ß-tubulin heterodimers and induce apoptotic cell death, maybe via phosphorylation of proteins regulating microtubule dynamics.

Dynamics of microtubules, which are composed of α/ß tubulin heterodimers, are regulated by microtubule-stabilizing and microtubule-destabilizing factors. Although phosphorylation of these factors contributes to regulation of microtubule dynamics, phosphorylation of tubulin itself is also involved. Cyclin-dependent kinase 1 phosphorylates ß-tubulin, and phosphorylated ß-tubulin regulates microtubule dynamics during mitosis [47]. Therefore, the author examined whether DAPK2 also phosphorylates ß-tubulin. However, an *in vitro* kinase assay revealed that DAPK2 failed to phosphorylate ß-tubulin, although MLC2, which is an

established substrate for DAPK2, was phosphorylated (data not shown). On the other hand, DAPK1 regulates the microtubule-associated protein tau through tau Thr^{231} and Pin1 phosphorylation, resulting in inhibition of microtubule assembly [60]. DAPK1 inhibits the prolyl isomerase activity of Pin1 through phosphorylation at Ser^{71} (-QSRRP$\underline{S^{71}}$S). A more recent study showed that the phospho-RXRXXpS/T antibody detected a binding partner of target of rapamycin Raptor when it was phosphorylated by DAPK2 [30], suggesting that DAPK2 may specifically recognize and phosphorylate the sequence RXXpS/T. DAPK2 may also regulate microtubule-associated proteins including tau via phosphorylation of Pin1 at Ser^{71}, leading to regulation of microtubule dynamics.

In conclusion, the author identified tubulin as an interacting partner of DAPK2. DAPK2 is involved in nocodazole-induced apoptosis (maybe via regulation of microtubule dynamics). Further investigations on not only interacting partners but also substrates of DAPK2 will elucidate the molecular mechanisms underlying DAPK2-induced apoptosis.

Chapter 4. Summary

The death-associated protein kinase (DAPK) family including DAPK1 and DAPK2 is a group of highly related serine/threonine kinases that are associated with a wide spectrum of apoptosis signals. But, mechanisms of cell apoptosis induction and regulations of the family, especially DAPK2, are not clear. In this study, the author focused on DAPK2 regulation and mechanism of DAPK2-induced apoptosis.

First, the author identified DAPK2 as a substrate of cGMP-dependent protein kinase (cGK). cGK has apoptosis inducibility, but substrates of cGK in apoptosis induction are not well known. The author performed global analysis using protein microarray, and identified DAPK2 as a novel substrate of cGK. cGK phosphorylate DAPK2 at Ser^{299}, Ser^{367} and Ser^{368}. Phosphorylation of DAPK2 Ser^{299} elevates its kinase activity. Phosphorylation of the residue can cancel autoinhibition by autophosphorylation. Moreover, phospho-mimic mutant DAPK2 S299D has 2-fold apoptosis inducibility compared with wild type in human breast cancer MCF-7 cells. Thus, cGK induces apoptosis via DAPK2 activation by phosphorylation.

Second, the author tried to reveal mechanism of DAPK2-induced apoptosis. The author identified ß-tubulin as a novel interaction partner of DAPK2 in HeLa cells. ß-tubulin is a one of component of microtubule. Polymer of α/ß tubulin heterodimers is microtubule. DAPK2 binds ß-tubulin via C-terminal region of DAPK2. Nocodazole, is an apoptosis inducer, is an inhibitor of α/ß tubulin polymerization. DAPK2-ß-tubulin interaction is enhanced by nocodazole-treatment. Furthermore, knockdown of DAPK2 inhibits nocodazole-induced apoptosis. Thus, DAPK2 mediates nocodazole-induced apoptosis through interaction with ß-tubulin.

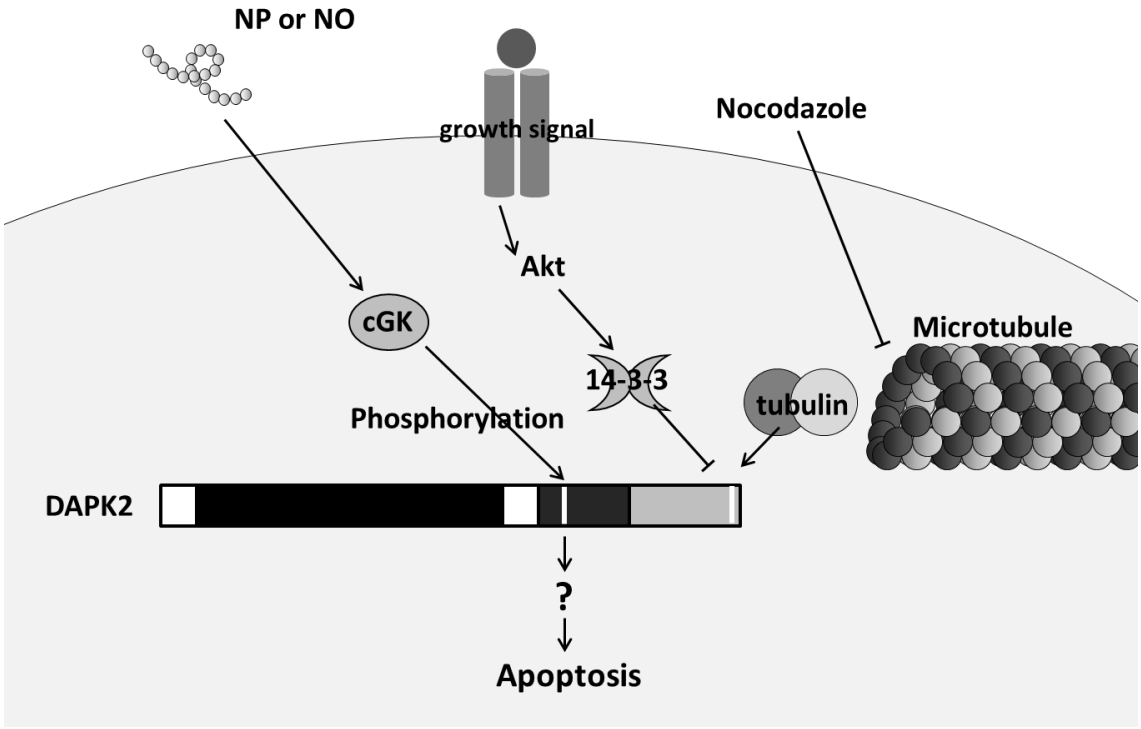
NP or NO
growth signal
Nocodazole
Akt
cGK
Microtubule
14-3-3
tubulin
Phosphorylation
DAPK2
?
Apoptosis

Chapter 5. Acknowledgment

This study was supported in part by Grant-in-Aid for Japan Society for the Promotion of Science (JSPS) Fellows (13J08248).

I would like to thank Prof. Akihiko Tsuji and Prof. Keizo Yuasa for their support of this research project and my graduate education. I wish to express my gratitude to the members of my committee, Prof. Hideaki Nagamune and Prof. Yoshitoshi Nakamura, for comments on this work.

I wish to thank Ms. Tokue Kuroda for experiments using radio isotope and Ms. Yuka Sasaki for protein identification by MALDI-TOF MS analysis. I am grateful to Mr. Taishi Hirase and Mr. Shinya Matsuda for technical assistance.

Finally, grate thanks to all my collaborators in laboratory of Prof. Tsuji's laboratory.

Chapter 6. References

[1] X-Z. Wu, A new classification system of anticancer drugs - based on cell biological mechanisms, Med. Hypotheses 66 (2006) 883–887.

[2] E.K. Rowinsky, R.C. Donehower, Paclitaxel (Taxol), N. Engl. J. Med. 332 (1995) 1004-1014.

[3] S. Elmore, Apoptosis: A review of programmed cell death, Toxicol. Pathol. 35 (2007) 495–516.

[4] Y. Tsujimoto, L.R. Finger, J. Yunis, P.C. Nowell, C.M. Croce, Cloning of the chromosome breakpoint of neoplastic B cells with the t(14;18) chromosome translocation, Science 226 (1984) 1097-1099.

[5] D. Hockenbery, G. Nuñez, C M illiman, R.D. Schreiber, S.J. Korsmeyer, Bcl-2 is an inner mitochondrial membrane protein that blocks programmed cell death, Nature 348 (1990) 334-336.

[6] A.J. Levine, J. Momand, C.A. Finlay, The p53 tumour suppressor gene, Nature 351 (1991) 453-456.

[7] A. Degterev, J. Yuan, Expansion and evolution of cell death programmes, Nat. Rev. Mol. Cell Biol. 9 (2008) 378–390.

[8] M. Casted, J-L. Perfettini, T. Roumier, K. Andreau, R. Medema, G. Kroemer, Cell death by mitotic catastrophe: a molecular definition, Oncogene 23 (2004) 2825–2837.

[9] K.E. Gascoigne, S.S. Taylor, How do anti-mitotic drugs kill cancer cells? J. Cell Sci. 122 (2009) 2579-2585.

[10] O. Cohen, E. Feinstein, A. Kimchi, DAP-kinase is a Ca^{2+}/calmodulin-dependent, cytoskeletal-associated protein kinase, with cell death-inducing functions that depend on its catalytic activity, EMBO J.16 (1997) 998–1008.

[11] B. Inbal, G. Shani, O. Cohen, J.L. Kissil, A. Kimchi, Death-associated protein kinase-related protein 1, a novel serine/threonin kinase involved in apoptosis, Mol. Cell Biol. 20 (2000) 1044-1054.

[12] T. Kawai, M. Matsumoto, K. Takeda, H. Sanjo, S. Akira, ZIP kinase, a novel serine/threonine kinase which mediates apoptosis, Mol. Cell Biol. 18 (1988) 1642-1651.

[13] D. Gozuacik, A. Kimchi, DAPk protein family and cancer, Autophagy 2 (2006) 74–79.

[14] R. Shiloh, S. Bialik, A. Kimchi, The DAPK family: a structure–function analysis, Apoptosis 19 (2014) 286–297.

[15] K. Yuasa, R. Ota, S. Matsuda, K. Isshiki, M. Inoue, A. Tsuji, Suppression of death-associated protein kinase 2 by interaction with 14-3-3 proteins, Biochem. Biophys. Res. Commun. 464 (2015) 70–75.

[16] Y. Huang, L. Chen, L. Guo, T.R. Hupp, Y. Lin, Evaluating DAPK as a therapeutic target, Apoptosis 19 (2014) 371–386

[17] B. Inbal, S. Bialik, I. Sabanay, G. Shani, A. Kimchi, DAP kinase and DRP-1 mediate membrane blebbing and the formation of autophagic vesicles during programmed cell death, J. Cell Biol. 157 (2002) 455–468.

[18] J. Ivanovska, V. Mahadevan, R. Schneider-Stock, DAPK and cytoskeleton-associated functions, Apoptosis 19 (2014) 329–338.

[19] V. Levin-Salomon, S. Bialik, A. Kimchi, DAP-kinase and autophagy, Apoptosis 19 (2014) 346–356.

[20] S. Bialik, A. Kimchi, The DAP-kinase interactome, Apoptosis 19 (2014) 316–328.

[21] T.H. Lee, C-H Chen, F. Suizu, P. Huang, C. Schiene-Fischer, S. Daum, Y.J. Zhang, A. Goate, R-H Chen, X.Z. Zhou, K.P. Lu, Death-associated protein kinase 1 phosphorylates Pin1 and inhibits its prolyl isomerase activity and cellular function, Mol. Cell 42 (2011) 147–159

[22] W-J Wang, J-C Kuo, W. Ku, Y-R Lee, F-C Lin, Y-L Chang, Y-M Lin, C-H Chen, Y-P Huang, M-J Chiang, S-W Yeh, P-R Wu, C-H Shen, C-T Wu, R-H Chen, The tumor suppressor DAPK is reciprocally regulated by tyrosine kinase Src and phosphatase LAR, Mol. Cell 27 (2007) 701–716.

[23] K. Bajbouj, A. Poehlmann, D. Kuester, T. Drewes, K. Haase, R. Hartig, A. Teller, S. Kliche, D. Walluscheck, J. Ivanovska, S. Chakilam, A. Ulitzsch, U. Bommhardt, M. Leverkus, A. Roessner, R. Schneider-Stock, Identification of phosphorylated p38 as a novel DAPK-interacting partner during TNF-induced apoptosis in colorectal tumor cells, Am. J. Physiol. 175 (2009) 557–570.

[24] A.L. Craig, J.A. Chrystal, J.A. Fraser, N. Sphyris, Y. Lin, B.J. Harrison, M.T. Scott, I. Dornreiter, T.R. Hupp, The MDM2 ubiquitination signal in the DNA-binding domain of p53 forms a docking site for calcium calmodulin kinase superfamily members, Mol. Cell Biol. 27 (2007) 3542–3555.

[25] T. Raveh, G. Droguett, M.S. Horwitz, R.A. DePinho, A. Kimchi, DAP kinase activates a p19ARF/p53-mediated apoptotic checkpoint to suppress oncogenic transformation, Nat. Cell Biol. 3 (2001) 1–7.

[26] W-J Wang, J-C Kuo, C-C Yao, R-H Chen, DAP-kinase induces apoptosis by suppressing integrin activity and disrupting matrix survival signals, J. Cell Biol. 159 (2002) 169–179.

[27] D. H. Weitzel, J. Chambers, T.A.J. Haystead, Phosphorylation-dependent control of ZIPK nuclear import is species specific, Cell. Signal. 23 (2011) 297–303.

[28] T. Usui, M. Okada, H. Yamawaki, Zipper interacting protein kinase (ZIPK): function and signaling, Apoptosis 19 (2014) 387–391.

[29] N. Sato, T. Kawai, K. Sugiyama, R. Muromoto, S. Imoto, Y. Sekine, M. Ishida, S. Akira, T. Matsuda, Physical and functional interactions between STAT3 and ZIP kinase, Int. Immunol. 17 (2005) 1543–1552.

[30] Y. Ber, R. Shiloh, Y. Gilad, N. Degani, S. Bialik, A. Kimchi, DAPK2 is a novel regulator of mTORC1 activity and autophagy, Cell Death Differ. 22 (2015) 465–475.

[31] S.M. Lohmann, A.B. Vaandrager, A. Smolenski, U. Walter, H.R. De Jonge, Distinct and specific functions of cGMP-dependent protein kinases, Trends Biochem. Sci. 22 (1997) 307–312.

[32] T. Shimojo, M. Hiroe, S. Ishiyama, H. Ito, T. Nishikawa, F. Marumo, Nitric oxide induces apoptotic death of cardiomyocytes via cyclic-GMP-dependent pathway, Exp. Cell Res. 247 (1999) 38–47.

[33] A. Deguchi, W.J. Thompson, I.B. Weinstein, Activation of protein kinase G is sufficient to induce apoptosis and inhibit cell migration in colon cancer cells, Cancer Res. 64 (2004) 3966–3973.

[34] I.K. Kwon, P.V. Schoenlein, J. Delk, K. Liu, M. Thangaraju, N.O. Dulin, V Ganapathy, F.G. Berger, D.D. Browning, Expression of cyclic guanosine monophosphate-dependent protein kinase in metastatic colon carcinoma cells blocks tumor angiogenesis, Cancer 112 (2008) 1462–1470.

[35] F. Fallahian, F. Karami-Tehrani, S. Salami, M. Aghaei, Cyclic GMP induced apoptosis via protein kinase G in oestrogen receptor-positive and –negative breast cancer cell lines, FEBS J. 278 (2011) 3360–3369.

[36] F. Fallahian, F. Karami-Tehrani, S. Salami, Induction of apoptosis by type Iß protein kinase G in the human breast cancer cell lines MCF-7 and MDA-MB-468, Cell Biochem. Funct. 30 (2011) 183–190.

[37] Y. Hou, N. Gupta, P. Schoenlein, E. Wong, R. Martindale, V. Ganapathy, D.D. Browning, An anti-tumor role for cGMP-dependent protein kinase, Cancer Lett. 240 (2006) 60–68.

[38] Y. Hou, E. Wong, J. Martin, P.V. Schoenlein, W.R. Dostmann, D.D. Browning, A role for cyclic-GMP dependent protein kinase in anoikis, Cell. Signal. 18 (2006) 882–888.

[39] I.K. Kwon, R. Wang, M. Thangaraju, H. Shuang, K. Liu, R. Dashwood, N. Dulin, V. Ganapathy, D.D. Browning, PKG inhibits TCF signaling in colon cancer cells by blocking ß-catenin expression and activating FOXO4, Oncogene 29 (2010) 3423–3434.

[40] J.W. Soh, Y. Mao, M.G. Kim, R. Pamukcu, H. Li, G.A. Piazza, W.J. Thompson, I.B. Weinstein, Cyclic GMP mediates apoptosis induced by sulindac derivatives via activation of c-Jun NH2-terminal kinase 1, Clin. Cancer Res. 6 (2000) 4136–4141.

[41] H.N. Tinsley, B.D. Gary, A.B. Keeton, W. Lu, Y. Li, G.A. Piazza, Inhibition of PDE5 by sulindac sulfide selectively induces apoptosis and attenuates oncogenic Wnt/ß-catenin-mediated transcription in human breast tumor cells, Cancer Prev. Res. 4 (2011) 1275–1284.

[42] K. Kinoshita, B. Habermann, A.A. Hyman, XMAP215: a key component of the dynamic microtubule cytoskeleton, Trends Cell Biol. 12 (2002) 267–273.

[43] V. Mennella, G.C. Rogers, S.L. Rogers, D.W. Buster, R.D. Vale, D.J. Sharp, Functionally distinct kinesin-13 family members cooperate to regulate microtubule dynamics during interphase, Nat. Cell Biol. 7 (2005) 235 – 245.

[44] L. Cassimeris, The oncoprotein 18/stathmin family of microtubule destabilizers, Curr. Opin. Cell Biol. 14 (2002) 18–24.

[45] P. Singh, K. Rathinasamy, R. Mohan, D. Panda, Microtubule assembly dynamics: an attractive target for anticancer drugs, IUBMB Life 60 (2008) 368-375.

[46] C. Dong, Z. Li, R. Alvarez Jr, X.H. Feng, P.J. Goldschmidt-Clermont, Microtubule binding to Smads may regulate TGFß activity, Mol. Cell 5 (2000) 27-34.

[47] A. Fourest-Lieuvin, L. Peris, V. Gache, I. Garcia-Saez, C. Juillan-Binard, V. Lantez, D. Job, Microtubule regulation in mitosis: tubulin phosphorylation by the cyclin-dependent kinase Cdk1, Mol. Biol. Cell 17 (2006) 1041-1050.

[48] K. Yuasa, T. Matsuda, A. Tsuji, Functional regulation of transient receptor potential canonical 7 by cGMP-dependent protein kinase Iα, Cell. Signalling 23 (2011) 1179-1187.

[49] L.P. Deiss, E. Feinstein, H. Berissi, O. Cohen, A. Kimchi, Identification of a novel serine/threonine kinase and a novel 15-kD protein as potential mediators of the gamma interferon-induced cell death, Genes Dev. 9 (1995) 15-30.

[50] T. Kawai, F. Nomura, K. Hoshino, N.G. Copeland, D.J. Gilbert, N.A. Jenkins, S. Akira, Death-associated protein kinase 2 is a new calcium/calmodulin dependent protein kinase that signals apoptosis through its catalytic activity, Oncogene 18 (1999) 3471-3480.

[51] G. Shani, S. Henis-Korenblit, G. Jona, O. Gileadi, M. Eisenstein, T. Ziv, A. Admon, A. Kimchi, Autophosphorylation restrains the apoptotic activity of DRP-1 kinase by controlling dimerization and calmodulin binding, EMBO J. 20 (2001) 1099-1113.

[52] R. Anjum, P.P. Roux, B.A. Ballif, S.P. Gygl, J. Blenis, The tumor suppressor DAP kinase is a target of RSK-mediated survival signaling, Curr. Biol. 15 (2005) 1762-1767.

[53] G. Shohat, T. Spivak-Kroizman, O. Cohen, S. Bialik, G. Shani, H. Berrisi, M. Eisenstein, A. Kimchi, The pro-apoptotic function of death-associated protein kinase is controlled by a unique inhibitory autophosphorylation-based mechanism, J. Biol. Chem. 276 (2001) 47460-47467.

[54] A.K. Patel, R.P. Yadav, V. Majava, I. Kursula, P. Kursula, Structure of dimeric autoinhibited conformation of DAPK2, a pro apoptotic protein kinase, J. Mol. Biol. 409 (2011) 369-383.

[55] H. Li, G. Ray, B.H. Yoo, M. Erdogan, K.V. Rosen, Down-regulation of death associated protein kinase-2 is required for ß-catenin-induced anoikis resistance of malignant epithelial cells, J. Biol. Chem. 284 (2009) 2012-2022.

[56] K. Isshiki, S. Matsuda, A. Tsuji, K. Yuasa, cGMP-dependent protein kinase I promotes cell apoptosis through hyperactivation of death-associated protein kinase 2, Biochem. Biophys. Res. Commun. 422 (2012) 280–284.

[57] Y. Gilad, R. Shiloh, Y. Ber, S. Bialik, A. Kimchi, Discovering protein-protein interactions within the programmed cell death network using a protein-fragment complementation screen, Cell Rep. 8 (2014) 909-921.

[58] M. Tewari, L.T. Quan, K. O'Rourke, S. Desnoyers, Z. Zeng, D.R. Beidler, G.G. Poirier, G.S. Salvesen, V.M. Dixit, Yama/CPP32 beta, a mammalian homolog of CED-3, is a CrmA-inhibitable protease that cleaves the death substrate poly(ADP-ribose) polymerase, Cell 81 (1995) 801-809.

[59] S.L. Mironov, M.V. Ivannikov, M. Johansson, $[Ca^{2+}]_i$ signaling between mitochondria and endoplasmic reticulum in neurons is regulated by microtubules from mitochondrial permeability transition pore to Ca^{2+}-induced Ca^{2+} release, J. Biol. Chem. 280 (2005) 715–721.

[60] B.M. Kim, M.H. You, C.H. Chen, S. Lee, Y. Hong, Y. Hong, A. Kimchi, X.Z. Zhou, T.H. Lee, Death-associated protein kinase 1 has a critical role in aberrant tau protein regulation and function, Cell Death Dis. 5 (2014) e1237.

Chapter 7. Appendix

List of publications

I.

cGMP-dependent protein kinase I promotes cell apoptosis through hyperactivation of death-associated protein kinase 2.

Biochem. Biophys. Res. Commun. 422 (2012) 280-284.

K. Isshiki, S. Matsuda, A. Tsuji, K. Yuasa.

II.

Death-associated protein kinase-2 mediates nocodazole-induced apoptosis through interaction with tubulin.

Biochem. Biophys. Res. Commun. 468 (2015) 113-118.

K. Isshiki, T. Hirase, K. Miyamoto, A. Tsuji, K. Yuasa.

I.

cGMP-dependent protein kinase I promotes cell apoptosis through hyperactivation of death-associated protein kinase 2.

Biochem. Biophys. Res. Commun. 422 (2012) 280-284.

K. Isshiki, S. Matsuda, A. Tsuji, K. Yuasa.

Biochemical and Biophysical Research Communications 422 (2012) 280–284

Contents lists available at SciVerse ScienceDirect

Biochemical and Biophysical Research Communications

journal homepage: www.elsevier.com/locate/ybbrc

cGMP-dependent protein kinase I promotes cell apoptosis through hyperactivation of death-associated protein kinase 2

Kinuka Isshiki, Shinya Matsuda, Akihiko Tsuji, Keizo Yuasa *

Department of Biological Science and Technology, The University of Tokushima Graduate School, Tokushima 770-8506, Japan

ARTICLE INFO

Article history:
Received 21 April 2012
Available online 3 May 2012

Keywords:
cGMP
cGK
DAPK2
Apoptosis

ABSTRACT

cGMP-dependent protein kinase-I (cGK-I) induces apoptosis in various cancer cell lines. However, the signaling mechanisms involved remain unknown. Using protein microarray technology, we identified a novel cGK substrate, death-associated protein kinase 2 (DAPK2), which is a Ca^{2+}/calmodulin-regulated serine/threonine kinase. cGK-I phosphorylated DAPK2 at Ser^{299}, Ser^{367} and Ser^{368}. Interestingly, a phospho-mimic mutant, DAPK2 S299D, significantly enhanced its kinase activity in the absence of Ca^{2+}/calmodulin, while a S367D/S368D mutant did not. Overexpression of DAPK2 S299D also resulted in a twofold increase in apoptosis of human breast cancer MCF-7 cells as compared with wild-type DAPK2. These results suggest that DAPK2 is one of the targets of cGK-I in apoptosis induction.

1. Introduction

The intracellular second messenger cGMP is generated by guanylate cyclases in response to natriuretic peptides and nitric oxide (NO), and primarily activates cGMP-dependent protein kinase (cGK, PKG). Two genes encoding for cGK-I and cGK-II have been identified, of which cGK-I has two splicing isoforms: cGK-Iα and cGK-Iβ [1]. cGMP/cGK signaling has been shown to be associated with anti-tumor activities, including induction of apoptosis and inhibition of metastasis and angiogenesis in many cell types [2–4]. Treatment of human breast cancer cell lines, MCF-7 and MDA-MB-468, with a cell-membrane permeable cGMP analog resulted in cell growth inhibition and apoptosis induction [5,6]. On the other hand, the expression of cGK-I isoforms is reduced in many tumors compared to normal tissues, and ectopic expression of cGK-Iβ results in decreased tumor growth and invasiveness in nude mouse xenografts [6]. In addition, ectopic expression of cGK-I isoforms in the human colon carcinoma lines SW480 and SW620, which do not express endogenous cGK-I, promoted anoikis (apoptosis resulting from a loss of cell–matrix interactions) [7]. A pro-apoptotic drug exisulind, an inhibitor of cGMP phosphodiesterase PDE5, increased intracellular cGMP levels in SW480 cells [8]. Furthermore, exisulind treatment resulted in induction of cGK-Iβ protein expression in addition to enzyme activation. Thus, it is highly likely that cGK activation is correlated with tumor cell apoptosis. Although recent studies suggested the involvement of the oncogene β-catenin and c-jun N-terminal kinase in cGMP/cGK-induced apoptosis [9–11], the detailed mechanism remains unknown.

The death-associated protein kinase (DAPK) family is a group of highly related serine/threonine kinases that are associated with a wide spectrum of apoptotic signals including interferon γ, tumor necrosis factor-α and anoikis [12]. The DAPK family consists of five members: DAPK1, DAPK2/DRP-1, DAPK3/ZIPK/DLK, DRAK1 and DRAK2. DAPK family members show high sequence homology in their N-terminal catalytic domains, while the structures of their C-terminal regions are different [13]. Both DAPK1 and DAPK2 possess a Ca^{2+}/calmodulin (CaM)-binding domain, while DAPK3 lacks this domain but has a leucine zipper domain and two nuclear localization signals. Although both DAPK1 and DAPK2 are activated by Ca^{2+}/CaM, autophosphorylation in their CaM-binding domains reduces their binding affinity for CaM and their activities [12,14]. In contrast, DAPK3 activity is enhanced by autophosphorylation [15]. Additionally, some members of the DAPK family are transcriptionally regulated by tumor suppressors and are frequently silenced by hypermethylation of their promoter regions in various cancers [13]. Recent studies have shown DAPK2 to be down-regulated in malignant epithelial cells by β-catenin and involved in anoikis [16].

In this study, we identified DAPK2 as a novel substrate for cGK-I using a protein microarray. cGK-I phosphorylated DAPK2 at Ser^{299}, Ser^{367} and Ser^{368}. Phosphorylation of DAPK2 at Ser^{299} enhanced its kinase activity. Furthermore, overexpression of a phospho-mimic DAPK2 mutant, DAPK2 S299D, strongly induced apoptosis in human breast cancer MCF-7 cells compared with wild-type DAPK2.

Abbreviations: cGK, cGMP-dependent protein kinase; DAPK, death-associated protein kinase; NO, nitric oxide; CaM, calmodulin; MLC, myosin light chain; GST, glutathione S-transferase; PBS, phosphate-buffered saline; GFP, green fluorescent protein; APC, adenomatous polyposis coli.

* Corresponding author. Fax: +81 88 655 3161.
E-mail address: yuasa@bio.tokushima-u.ac.jp (K. Yuasa).

0006-291X/$ - see front matter © 2012 Elsevier Inc. All rights reserved.
http://dx.doi.org/10.1016/j.bbrc.2012.04.148

These findings highlight the importance of the cGK-I/DAPK2 signaling pathway in regulating apoptosis.

2. Materials and methods

2.1. Plasmid construction

cDNAs encoding mouse myosin light chain 2 (MLC2) and mouse DAPK2 were cloned by PCR using the respective specific primers. PCR products were cloned into TA-cloning vector pGEM-T Easy (Promega), and the inserted DNA sequences were confirmed by DNA sequencing. A cDNA encoding for mouse DAPK2 was subcloned into the mammalian expression vector pFLAG-CMV-2 (Sigma). A cDNA encoding for mouse MLC2 was subcloned into a glutathione S-transferase (GST) expression vector, pGEX (GE Healthcare). Site-directed mutagenesis was performed using PrimeSTAR Mutagenesis Basal Kit (Takara Bio) according to the manufacturer's instructions. The mutation was confirmed by DNA sequencing analysis.

2.2. Cell culture and transfection

COS-7 and MCF-7 cells were cultured in Dulbecco's modified Eagle's medium supplemented with 10% fetal bovine serum, 100 units/ml penicillin and 100 μg/ml streptomycin at 37 °C in 5% CO_2. Transfection was performed using Lipofectamine 2000 (Invitrogen), according to the manufacturer's instructions.

2.3. Protein microarray

ProtoArray Human Protein Microarray Kinase Substrate Identification (KSI) Complete Kit (Invitrogen) was used according to the manufacturer's instructions. After equilibration at 4 °C for 15 min, the arrays were blocked with 1% bovine serum albumin in phosphate-buffered saline (PBS) for 2 h at 4 °C. 120 μl of kinase buffer [100 mM MOPS, pH 7.2, 1% Nonidet P40, 100 mM NaCl, 10 mg/ml BSA, 5 mM $MgCl_2$, 5 mM $MnCl_2$, 1 mM dithiothreitol and 10 μCi/μl of [γ-^{33}P]ATP (33 nM final concentration) (Perkin Elmer)] containing 50 nM purified bovine cGK-Iα (Promega) and 5 μM cGMP was overlaid onto the array and incubated for 1 h at 30 °C. As a negative control, buffer was overlaid onto the array. The arrays were washed twice with 0.5% SDS and twice with H_2O at room temperature, dried and exposed to X-ray films. Spots were identified using GenePix Pro (Molecular Devices).

2.4. In vitro kinase assay

In vitro phosphorylation by cGK-I was performed as previously described [17]. MLC2 was used as a substrate for a DAPK2 activity assay. GST–MLC2 fusion protein was expressed in *Escherichia coli* and purified as previously described [17]. COS-7 cells transfected with pFLAG-DAPK2 wild type or mutant, were harvested with TNE buffer (20 mM Tris–HCl pH 7.5, 150 mM NaCl, 1% NP-40 and 1 mM EDTA) supplemented with protease inhibitors (10 μg/ml leupeptin and 10 μg/ml aprotinin). Cell lysates were incubated with an anti-FLAG M2 antibody (Sigma) and protein G Sepharose (GE Healthcare) overnight at 4 °C. The beads were washed three times with TNE buffer and twice with 50 mM Tris–HCl, pH7.5. The kinase reaction was carried out by resuspending the complexes in 100 μl of kinase buffer [50 mM Tris–HCl pH 7.5, 20 mM magnesium acetate, 100 μM or 50 μM ATP, 2 μCi [γ-^{32}P]ATP, phosphatase inhibitor cocktail (Nacalai Tesque) and 30 μg/ml purified GST–MLC2] including either 100 mM $CaCl_2$ and 10 nM CaM, or 5 mM EGTA, and incubating for 30 min at 30 °C. Phosphorylated GST–MLC2 was separated by SDS–PAGE and visualized with a BAS-1500 Bioimaging Analyzer (Fuji Film). Quantitative densitometric analysis was performed using Image J.

2.5. Analysis of apoptosis

MCF-7 cells were transiently transfected with either FLAG-tagged DAPK2 wild type or mutants together with a green fluorescent protein (GFP) plasmid. Twenty-four hours after transfection, cells were stained with Hoechst 33342 (Invitrogen) for 10 min at 37 °C in 5% CO_2. They were washed with PBS and fixed with 3.7% formaldehyde in PBS for 30 min at room temperature. After washing with PBS, GFP-expressing cells were observed with a fluorescence microscope (IX71, Olympus). The number of apoptotic cells displaying both membrane blebbing and nuclear condensation was counted and expressed as a percentage of the total cell number; a minimum of 50 randomly chosen cells were counted for each sample.

3. Results

3.1. Identification of putative substrates for cGK-I by protein microarray analysis

To identify novel cGK substrates implicated in inducing apoptosis, we used a human protein microarray spotted with 1700

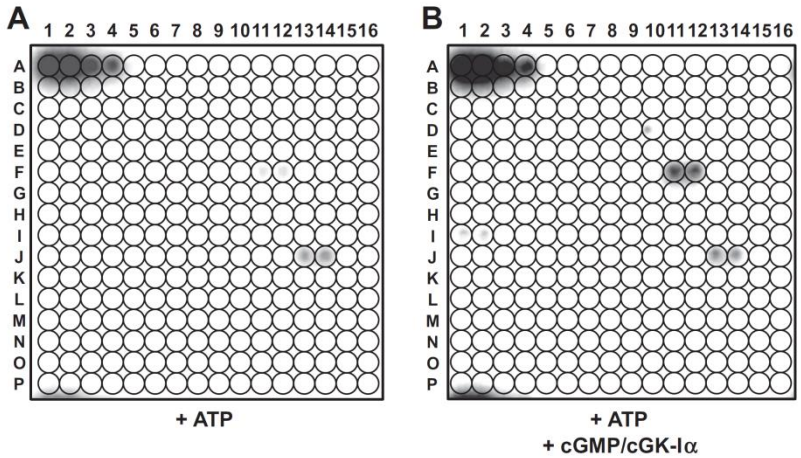

Fig. 1. Identification of DAPK2 as a putative substrate for cGK-I by protein microarray analysis. Human protein microarrays were incubated with [γ-^{33}P]ATP in the absence (A) or presence (B) of cGMP/cGK-Iα. After 30 min, the arrays were dried and exposed to X-ray films. At positions A1–4 and J13–14, protein kinases were autophosphorylated in the presence of ATP. Positions F11–12 were spotted with GST–DAPK2.

GST-tagged proteins in duplicate. The microarrays were incubated with [γ-^{33}P]ATP in the presence or absence of cGMP/cGK-Iα. Spots A1–4 and J13–14 on both arrays were protein kinases that were autophosphorylated in the presence of ATP (Fig. 1). Some spots with strong signals were found on the array incubated with cGMP and cGK-Iα (Fig. 1B) as compared with the control array (Fig. 1A). Spots F11–12, which were spotted with GST–DAPK2, showed greater than 20-fold differences in their signal intensities. DAPK2 is a Ca^{2+}/CaM-dependent protein kinase belonging to the DAPK family [18]. This family consists of five members and acts as a positive regulator of apoptosis [13,18–21]. Amino acid sequence analysis of human DAPK2 identified three potential phosphorylation sites, RRES^{299}, RRRS^{367} and RRSS^{368} for cGK (RR/KXS/T). These sequences are also conserved in mouse and rat DAPK2. These results suggested that DAPK2 was a putative substrate for cGK-I.

Amino acid sequence analysis of human DAPK1 indicated that DAPK1 also has some potential phosphorylation sites for cGK, suggesting that DAPK1 is also phosphorylated by cGK. However, we missed to identify DAPK1 as a novel substrate for cGK-I using protein microarray, because only small amount of GST–DAPK1 protein (nearly one-tenth of GST–DAPK2 protein) was spotted (data not shown).

3.2. cGK-Iβ phosphorylates DAPK2 at Ser^{299}, Ser^{367} and Ser^{368}

To confirm the protein microarray results, we investigated if cGK-I could phosphorylate DAPK2 in an *in vitro* kinase assay. COS-7 cells were transfected with FLAG-tagged mouse DAPK2 along with FLAG-tagged cGK-Iβ. Cell lysates were immunoprecipitated with an anti-FLAG antibody, and the immunocomplex was incubated with [γ-^{32}P]ATP in the presence or absence of cGMP. As shown in Fig. 2A, wild-type DAPK2 was phosphorylated even without cGMP and cGK-Iβ because DAPK2 was autophosphorylated as reported previously [18,21]. To detect cGMP/cGK-mediated phosphorylation of DAPK2, we produced a kinase-dead mutant, DAPK2 K52A, and assessed it with an *in vitro* kinase assay. DAPK2 K52A was not autophosphorylated, but was efficiently phosphorylated by cGK-Iβ in a cGMP-dependent manner (Fig. 2A). This confirmed that DAPK2 was phosphorylated by cGK-I *in vitro*.

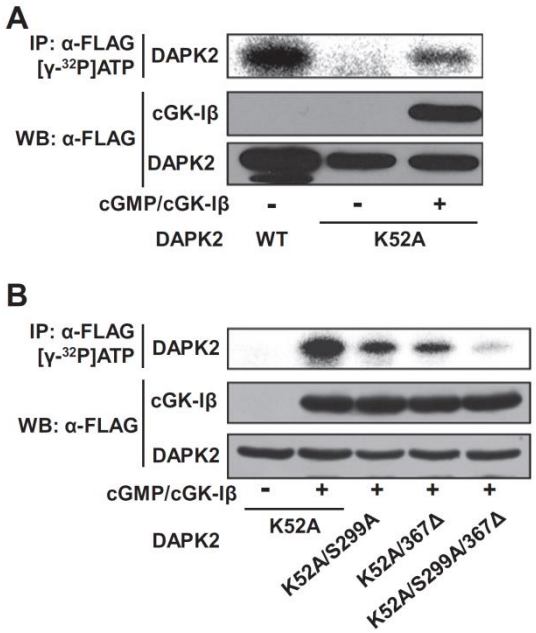

Fig. 2. cGK-I phosphorylates DAPK2 at Ser^{299}, Ser^{367} and Ser^{368}. (A and B) FLAG-tagged DAPK2 wild type or mutant was expressed in COS-7 cells along with FLAG-tagged cGK-Iβ. FLAG-tagged proteins were immunoprecipitated and incubated in a kinase buffer containing [γ-^{32}P]ATP with or without cGMP. To monitor the expression level of the FLAG-tagged proteins, cell lysates were blotted with an anti-FLAG antibody.

DAPK2 has three potential sites for phosphorylation by cGK: Ser^{299}, Ser^{367} and Ser^{368}. To identify DAPK2 sites phosphorylated by cGK-I, we created phospho-resistant mutants for these sites. Ser^{299} was replaced by non-phosphorylatable Ala (DAPK2 K52A/S299A). Because DAPK2 is a protein comprised of 370 amino acids and its Ser^{367} and Ser^{368} residues are close to the C-terminal end, Ser^{367} was replaced by a stop codon, DAPK2 K52A/367Δ. As shown in Fig. 2B, an *in vitro* kinase assay demonstrated that the phosphorylation of both DAPK2 K52A/S299A and K52A/367Δ by cGK-Iβ were reduced compared with that of DAPK2 K52A. Furthermore, cGK-Iβ failed to phosphorylate a triple mutant, DAPK2 K52A/S299A/367Δ. These results suggest that cGK-I phosphorylates DAPK2 at Ser^{299}, Ser^{367} and Ser^{368}.

3.3. Phosphorylation of DAPK2 at Ser^{299} by cGK-I increases its kinase activity

Next, we examined whether DAPK2 phosphorylation affects its kinase activity. Although the three putative phosphorylation sequences (RRES^{299}, RRRS^{367} and RRSS^{368}) were completely matched to the consensus motif for cGK (RR/KXS/T), RSST^{369} also partially corresponded to this phosphorylation motif. Thus, three phospho-mimic mutants were generated in which the putative cGK phosphorylation sites were replaced by Asp: DAPK2 S299D, DAPK2 S367D/S368D and DAPK2 S367D/S368D/T369D. Myosin light chain 2 (MLC2) was used as a substrate for DAPK activity as previously described [13]. As shown in Fig. 3A, wild-type DAPK2 phosphorylated GST–MLC2 in a Ca^{2+}/CaM-dependent manner (3.4-fold increase). Interestingly, the activity of the DAPK2 S299D mutant was significantly increased compared with that of the wild type in the presence of Ca^{2+}/CaM (twofold increase), whereas the activities of DAPK2 S367D/S368D and DAPK2 S367D/S368D/T369D mutants were not. In addition, the DAPK2 S299D mutant showed a significantly high activity even without Ca^{2+}/CaM. The activity of another phospho-mimic mutant, DAPK2 S299E, was also examined. As expected, the DAPK2 S299E mutant also exhibited enhanced kinase activity like that of the DAPK2 S299D mutant (Fig. 3B). These findings suggested that phosphorylation of DAPK2 at Ser^{299}, but not at Ser^{367} and Ser^{368}, stimulated its kinase activity independently of Ca^{2+}/CaM.

A previous study demonstrated that DAPK2 was autophosphorylated at Ser^{318} and inactivated, and that DAPK2 activation is required for dephosphorylation of Ser^{318} [12]. To examine whether phosphorylation of Ser^{299} affects autoinhibition by phosphorylation at Ser^{318}, we generated DAPK2 S318E and DAPK2 S299D/S318E mutants and examined their activities with an *in vitro* kinase assay. As shown in Fig. 3C, the DAPK2 S318E mutant was not activated by Ca^{2+}/CaM, consistent with a previous report [12]. On the other hand, the kinase activity of the DAPK2 S299D/S318E double mutant was similar to that of the DAPK2 S299D mutant and overcame the inhibitory effect of phosphorylation at Ser^{318}. These results suggested that DAPK2 phosphorylation at Ser^{299} increased its kinase activity by a Ca^{2+}/CaM-independent mechanism and also interfered with the autoinhibitory mechanism resulting from phosphorylation at Ser^{318}.

3.4. A phospho-mimic mutant DAPK2 S299D strongly induces apoptosis compared with wild-type DAPK2

A previous study showed that DAPK2 overexpression induced apoptosis in various cell lines, and that a dominant-negative

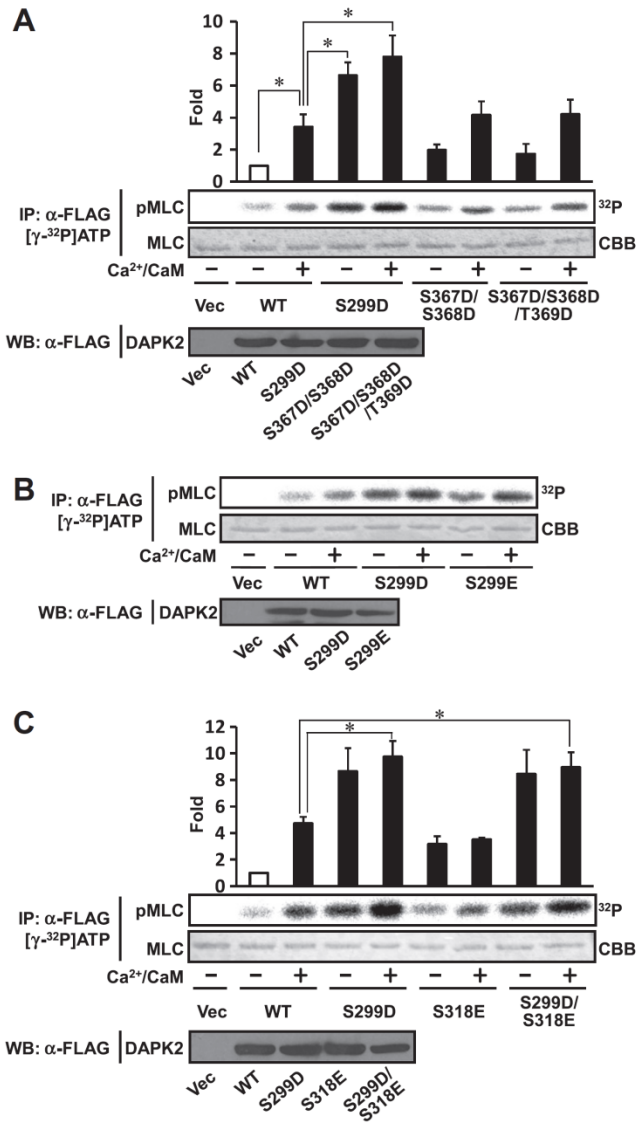

Fig. 3. Phosphorylation of DAPK2 at Ser^{299} enhances its kinase activity. (A, B and C) COS-7 cells were transiently transfected with FLAG-DAPK2 wild type or mutant. FLAG-DAPK2 proteins were immunoprecipitated and used in an *in vitro* kinase assay with recombinant GST–MLC2 as a substrate in the presence of either $CaCl_2$/CaM or EGTA. GST–MLC2 was separated on SDS–PAGE, after which the gel was analyzed by Coomassie blue staining and a bioimaging analyzer. The relative kinase activity of DAPK2 was quantified by densitometric analysis. The activity of wild-type DAPK2 without Ca^{2+}/CaM was taken as 1. All experiments were performed three times independently. Results are expressed as means ± S.E. Statistical significance was determined by Student's *t*-test. $^{*}P < 0.05$, $^{**}P < 0.01$.

DAPK2 mutant protected cells from TNF-α-induced apoptosis [18]. These results suggested a strong association between DAPK2 catalytic activity and apoptosis. Thus, we tested whether DAPK2 phosphorylation at Ser^{299} affected the induction of apoptosis in human breast cancer MCF-7 cells. In a previous study [22], apoptotic morphological changes, such as membrane blebbing and nuclear condensation, were clearly observed in MCF-7 cells that were transfected with DAPK2. We transiently transfected MCF-7 cells with either DAPK2 wild type or mutants along with GFP. In GFP-expressing cells, the number of apoptotic cells displaying both membrane blebbing and nuclear condensation was counted. As shown in Fig. 4, overexpression of wild-type DAPK2 significantly induced apoptosis, whereas a DAPK2 inactive mutant, S318E, induced fewer apoptotic changes than wild type consistent with a previous report [12]. In agreement with the data for kinase activity,

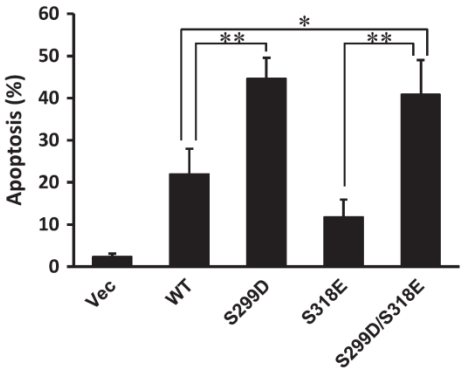

Fig. 4. Phospho-mimic mutant DAPK2 S299D enhances apoptosis induction in MCF-7 cells. pFLAG-DAPK2 wild type or mutant was transiently transfected into MCF-7 cells along with pEGFP. After 24 h, cells were stained with Hoechst 33342 and fixed with formaldehyde. Fixed cells were observed under a fluorescence microscope. The number of cells showing apoptotic morphologies was expressed as a percentage of the total number of GFP-expressing cells counted. Experiments were performed three times independently. Results are expressed as means ± S.E. Statistical significance was determined by Student's *t*-test. $^{*}P < 0.05$, $^{**}P < 0.01$.

forced expression of the phospho-mimic mutant DAPK2 S299D resulted in a twofold increase in apoptotic cells compared with wild-type DAPK2. In addition, the same result was observed for DAPK2 S299D/S318E-expresseing cells. These results suggested that cGK-I induced apoptosis through DAPK2 phosphorylation.

4. Discussion

cGMP/cGK signaling can induce apoptosis in cancer cell lines and it has been suggested that this signaling pathway could be a target for anti-cancer agents [2–4]. However, the detailed signaling mechanisms remain unclear. In this study, we identified DAPK2 as a novel cGK substrate using protein microarray technology. DAPK2 belongs to the DAPK family comprised of five kinases that share a high sequence homology in their catalytic domains and are involved in apoptosis induction. DAPK2 is a CaM-dependent serine/threonine kinase that is activated by CaM in response to Ca^{2+} stimuli. In addition to its activation by Ca^{2+}/CaM, DAPK2 activity is also regulated by an autoinhibitory mechanism. By the mechanism called a "double-locking" mechanism, DAPK2 is kept in an inactive state [12]. DAPK2 activation is required for dephosphorylation of an autophosphorylated residue Ser^{318} within the CaM-binding domain and for Ca^{2+}/CaM binding. The negative charge of its phospho-Ser^{318} residue interacts with the positive charge of a Lys^{151} residue in its active site, which results in the inhibition of CaM binding. This autoinhibitory mechanism is necessary to prevent erroneous activation in response to random fluctuations in cellular Ca^{2+} levels. We found that DAPK2 phosphorylation at Ser^{299} increased its kinase activity in a Ca^{2+}/CaM-independent manner and overcame the autoinhibitory mechanism resulting from phosphorylation at Ser^{318}. Because the Ser^{299} residue phosphorylated by cGK-I is also present in the CaM-binding domain and is close to the autophosphorylation Ser^{318} site, we suggest that DAPK2 phosphorylation at Ser^{299} could disrupt the interaction between phospho-Ser^{318} and Lys^{151} and promote Ca^{2+}/CaM binding, thus triggering DAPK2 hyperactivation. However, a CaM overlay assay revealed that a phospho-mimic mutation at Ser^{299} did not influence the binding of CaM to DAPK2 (data not shown). DAPK2 activity has also been shown to be regulated by dimerization [12,23]. This suggests that other mechanisms may be involved in the hyperactivation of DAPK2 by Ser^{299} phosphorylation. DAPK1 and DAPK2 show high sequence homology in their CaM binding domains and have conserved autophosphorylation sites [12,14]. Sequence alignments indicate that DAPK1 has a Ser^{289} residue cor-

responding to Ser^{299} in DAPK2. Interestingly, a previous study showed that DAPK1 phosphorylation at Ser^{289} by p90 ribosomal S6 kinase inhibited its pro-apoptotic activity in a non-tumor cell line, HEK293E [24]. However, our findings may be supported by another study that showed that DAPK2 was activated via trans-phosphorylation of residue(s) other than Ser^{318} by unidentified kinase(s) [12]. Because the autoinhibitory mechanism of DAPK2 has been shown to be different from that of DAPK1 [23], phosphorylation at Ser^{289} in DAPK1 and Ser^{299} in DAPK2 may exert opposite effects.

In cancer cell lines, the expression of DAPK2 is generally silenced by hypermethylation of its promoter [13]. However, a previous report showed that knockdown of oncogenic β-catenin by RNA interference induced DAPK2 expression in a colon cancer cell line [16]. This cell line lacked a functional adenomatous polyposis coli (APC) tumor suppressor protein. Although APC induces β-catenin degradation in normal cells, which is dependent on phosphorylation by glycogen synthase kinase 3β, its degradation is often blocked by loss-of-function mutations of APC in carcinomas. On the other hand, cGMP/cGK signaling attenuates β-catenin-mediated transcription but not β-catenin degradation in colon and breast cancer cells, although the downstream target(s) directly regulated by cGK remain unclear [9,11]. Taken together, cGMP/cGK-I signaling may increase DAPK2 expression via suppression of β-catenin-mediated transcription and activate DAPK2 via phosphorylation at Ser^{299}, resulting in induction of apoptosis in cancer cells.

In summary, we identified a novel cGK-I substrate implicated in apoptosis induction. We determined that DAPK2 kinase activity was regulated by its trans-phosphorylation. Phosphorylation of DAPK2 at Ser^{299} enhanced its kinase activity, which resulted in inducing apoptosis in MCF-7 cells. Further research is required to unravel the cGMP/cGK-I signaling mechanisms involved in order to develop more efficacious anti-tumor drugs.

Acknowledgments

The authors thank Mr. Taito Matsuda and Miss Kyoko Fukuda for their technical assistants. This work was supported in part by Grant-in-Aid for Young Scientists (B) from the Ministry of Education, Culture, Sports, Science, and Technology of Japan.

References

[1] S.M. Lohmann, A.B. Vaandrager, A. Smolenski, U. Walter, H.R. De Jonge, Distinct and specific functions of cGMP-dependent protein kinases, Trends Biochem. Sci. 22 (1997) 307–312.

[2] T. Shimojo, M. Hiroe, S. Ishiyama, H. Ito, T. Nishikawa, F. Marumo, Nitric oxide induces apoptotic death of cardiomyocytes via cyclic-GMP-dependent pathway, Exp. Cell Res. 247 (1999) 38–47.

[3] A. Deguchi, W.J. Thompson, I.B. Weinstein, Activation of protein kinase G is sufficient to induce apoptosis and inhibit cell migration in colon cancer cells, Cancer Res. 64 (2004) 3966–3973.

[4] I.K. Kwon, P.V. Schoenlein, J. Delk, K. Liu, M. Thangaraju, N.O. Dulin, V. Ganapathy, F.G. Berger, D.D. Browning, Expression of cyclic guanosine monophosphate-dependent protein kinase in metastatic colon carcinoma cells blocks tumor angiogenesis, Cancer 112 (2008) 1462–1470.

[5] F. Fallahian, F. Karami-Tehrani, S. Salami, M. Aghaei, Cyclic GMP induced apoptosis via protein kinase G in oestrogen receptor-positive and -negative breast cancer cell lines, FEBS J. 278 (2011) 3360–3369.

[6] F. Fallahian, F. Karami-Tehrani, S. Salami, Induction of apoptosis by type Iβ protein kinase G in the human breast cancer cell lines MCF-7 and MDA-MB-468, Cell Biochem. Funct. 30 (2011) 183–190.

[7] Y. Hou, N. Gupta, P. Schoenlein, E. Wong, R. Martindale, V. Ganapathy, D.D. Browning, An anti-tumor role for cGMP-dependent protein kinase, Cancer Lett. 240 (2006) 60–68.

[8] Y. Hou, E. Wong, J. Martin, P.V. Schoenlein, W.R. Dostmann, D.D. Browning, A role for cyclic-GMP dependent protein kinase in anoikis, Cell. Signalling 18 (2006) 882–888.

[9] I.K. Kwon, R. Wang, M. Thangaraju, H. Shuang, K. Liu, R. Dashwood, N. Dulin, V. Ganapathy, D.D. Browning, PKG inhibits TCF signaling in colon cancer cells by blocking β-catenin expression and activating FOXO4, Oncogene 29 (2010) 3423–3434.

[10] J.W. Soh, Y. Mao, M.G. Kim, R. Pamukcu, H. Li, G.A. Piazza, W.J. Thompson, I.B. Weinstein, Cyclic GMP mediates apoptosis induced by sulindac derivatives via activation of c-Jun NH_2-terminal kinase 1, Clin. Cancer Res. 6 (2000) 4136–4141.

[11] H.N. Tinsley, B.D. Gary, A.B. Keeton, W. Lu, Y. Li, G.A. Piazza, Inhibition of PDE5 by sulindac sulfide selectively induces apoptosis and attenuates oncogenic Wnt/β-catenin-mediated transcription in human breast tumor cells, Cancer Prev. Res. 4 (2011) 1275–1284.

[12] G. Shani, S. Henis-Korenblit, G. Jona, O. Gileadi, M. Eisenstein, T. Ziv, A. Admon, A. Kimchi, Autophosphorylation restrains the apoptotic activity of DRP-1 kinase by controlling dimerization and calmodulin binding, EMBO J. 20 (2001) 1099–1113.

[13] D. Gozuacik, A. Kimchi, DAPk protein family and cancer, Autophagy 2 (2006) 74–79.

[14] G. Shohat, T. Spivak-Kroizman, O. Cohen, S. Bialik, G. Shani, H. Berrisi, M. Eisenstein, A. Kimchi, The pro-apoptotic function of death-associated protein kinase is controlled by a unique inhibitory autophosphorylation-based mechanism, J. Biol. Chem. 276 (2001) 47460–47467.

[15] P.R. Graves, K.M. Winkfield, A.T. Haystead, Regulation of zipper-interacting protein kinase activity *in vitro* and *in vivo* by multisite phosphorylation, J. Biol. Chem. 280 (2005). 9363-9347.

[16] H. Li, G. Ray, B.H. Yoo, M. Erdogan, K.V. Rosen, Down-regulation of death associated protein kinase-2 is required for β-catenin-induced anoikis resistance of malignant epithelial cells, J. Biol. Chem. 284 (2009) 2012–2022.

[17] K. Yuasa, T. Matsuda, A. Tsuji, Functional regulation of transient receptor potential canonical 7 by cGMP-dependent protein kinase Iα, Cell. Signalling 23 (2011) 1179–1187.

[18] B. Inbal, G. Shani, O. Cohen, J.L. Kissil, A. Kimchi, Death-associated protein kinase-related protein 1, a novel serine/threonine kinase involved in apoptosis, Mol. Cell. Biol. 20 (2000) 1044–1054.

[19] L.P. Deiss, E. Feinstein, H. Berissi, O. Cohen, A. Kimchi, Identification of a novel serine/threonine kinase and a novel 15-kD protein as potential mediators of the gamma interferon-induced cell death, Genes Dev. 9 (1995) 15–30.

[20] T. Kawai, M. Matsumoto, K. Takeda, H. Sanjo, S. Akira, ZIP kinase, a novel serine/threonine kinase which mediates apoptosis, Mol. Cell. Biol. 18 (1988) 1642–1651.

[21] T. Kawai, F. Nomura, K. Hoshino, N.G. Copeland, D.J. Gilbert, N.A. Jenkins, S. Akira, Death-associated protein kinase 2 is a new calcium/calmodulin-dependent protein kinase that signals apoptosis through its catalytic activity, Oncogene 18 (1999) 3471–3480.

[22] B. Inbal, S. Bialik, I. Sabanay, G. Shani, A. Kimchi, DAP kinase and DRP-1 mediate membrane blebbing and the formation of autophagic vesicles during programmed cell death, J. Cell Biol. 157 (2002) 455–468.

[23] R. Anjum, P.P. Roux, B.A. Ballif, S.P. Gygl, J. Blenis, The tumor suppressor DAP kinase is a target of RSK-mediated survival signaling, Curr. Biol. 15 (2005) 1762–1767.

[24] A.K. Patel, R.P. Yadav, V. Majava, I. Kursula, P. Kursula, Structure of dimeric autoinhibited conformation of DAPK2, a pro apoptotic protein kinase, J. Mol. Biol. 409 (2011) 369–383.

II.

Death-associated protein kinase-2 mediates nocodazole-induced apoptosis through interaction with tubulin.

Biochem. Biophys. Res. Commun. 468 (2015) 113-118.

K. Isshiki, T. Hirase, K. Miyamoto, A. Tsuji, K. Yuasa.

Biochemical and Biophysical Research Communications 468 (2015) 113–118

Contents lists available at ScienceDirect

Biochemical and Biophysical Research Communications

journal homepage: www.elsevier.com/locate/ybbrc

Death-associated protein kinase 2 mediates nocodazole-induced apoptosis through interaction with tubulin

Kinuka Isshiki, Taishi Hirase, Shinya Matsuda, Kenji Miyamoto, Akihiko Tsuji, Keizo Yuasa*

Department of Biological Science and Technology, Tokushima University Graduate School, 2-1 Minamijosanjima, Tokushima 770-8506, Japan

ARTICLE INFO

Article history:
Received 10 October 2015
Accepted 28 October 2015
Available online 31 October 2015

Keywords:
DAPK2
Apoptosis
Tubulin
Nocodazole

ABSTRACT

Death-associated protein kinase 2 (DAPK2) is a positive regulator of apoptosis. Although we recently reported that 14-3-3 proteins inhibit DAPK2 activity and its subsequent apoptotic effects via binding to DAPK2, the molecular mechanisms underlying the DAPK2-mediated apoptotic pathway remain unclear. Therefore, we attempted to further identify DAPK2-interacting proteins using pull-down assays and mass spectrometry. The microtubule β-tubulin was identified as a novel DAPK2-binding protein in HeLa cells. Pull-down assays revealed that DAPK2 interacted with the α/β-tubulin heterodimer, and that the C-terminal region of DAPK2, which differs from that of other DAPK family members, was sufficient for the association with β-tubulin. Although the microtubule-depolymerizing agent nocodazole induced apoptosis in HeLa cells, the level of apoptosis was significantly decreased in the DAPK2 knockdown cells. Furthermore, we found that treatment with nocodazole resulted in an increased binding of DAPK2 to β-tubulin. These findings indicate that DAPK2 mediates nocodazole-induced apoptosis via binding to tubulin.

1. Introduction

The death-associated protein kinase (DAPK) family consists of five kinases, including DAPK1, DAPK2, and DAPK3, and plays an important role in cell death induced by a wide variety of apoptosis inducers, including interferon γ, tumor necrosis factor (TNF)-α, Fas ligand, and TNF-related apoptosis-inducing ligand [1–3]. The family possesses highly homologous N-terminal catalytic domains and diverse C-terminal domains. The variation in the C-terminal region suggests that the family members are controlled by different regulatory mechanisms and have distinct functions through different signaling pathways. DAPK1, the most well-studied member of the family, possesses a Ca^{2+}/calmodulin (CaM)-binding domain, eight ankyrin repeats, a cytoskeletal-binding domain, and a death domain at the C-terminal region. Binding of Ca^{2+}/CaM to the CaM-binding domain causes catalytic activation. On the other hand, the cytoskeletal-binding domain contributes to the subcellular localization of DAPK1 and consequently affects its physiological function, including the disruption of integrin signaling, promotion of anoikis, and suppression of cell motility [4,5]. DAPK3, also known as zipper-interacting protein kinase, contains two nuclear localization signals and a leucine zipper domain, which are involved in the nuclear localization and the interaction of DAPK3 with several transcriptional factors including activating transcription factor 4 and signal transducer and activator of transcription 3 [6]. Although DAPK2 shares a CaM-binding domain with DAPK1 and is activated by CaM in response to Ca^{2+} stimuli, its C-terminal region is short and does not include any other domains, such as the cytoskeletal-binding domain. Recently, we identified 14-3-3 proteins as the interaction partners of DAPK2 from human breast cancer MCF-7 cells [7]. 14-3-3 proteins bind to phosphorylated serine or threonine residues in defined consensus sequences. Interactions between 14-3-3 proteins and DAPK2 are dependent on the phosphorylation of Thr^{369} in the C-terminal region and effectively suppress DAPK2 kinase activity and DAPK2-induced apoptosis. However, the molecular mechanism of the DAPK2-mediated apoptotic signaling pathway remains to be elucidated.

Microtubules, which are composed of α/β-tubulin heterodimers, are a major component of the cytoskeleton. Microtubule dynamics (polymerization and depolymerization) are regulated by the

Abbreviations: DAPK, death-associated protein kinase; TNF, tumor necrosis factor; CaM, calmodulin; GST, glutathione S-transferase; MALDI-TOF MS, matrix-assisted laser desorption/ionization time-of-flight mass spectrometry; PARP, poly (ADP-ribose) polymerase.

* Corresponding author.
E-mail address: kyuasa@tokushima-u.ac.jp (K. Yuasa).

http://dx.doi.org/10.1016/j.bbrc.2015.10.151
0006-291X/

coordinated action of microtubule-stabilizing and -destabilizing factors and play an important role not only in cell migration and polarization but also in mitosis and the cell cycle, particularly the formation of the spindle apparatus. Antimicrotubule agents, including polymerizing (e.g., paclitaxel) and depolymerizing (e.g., vinca alkaloid and nocodazole) agents, interfere with these dynamic processes, resulting in apoptotic cell death. Therefore, several antimicrotubule agents are used as anticancer drugs [8]. Nocodazole is a well-known inhibitor of microtubule polymerization and arrests cell cycle progression at the G2/M-phase. Disruption of microtubules with nocodazole influences signal transduction events, such as the disruption of the complex between Smads and microtubules [9] and the phosphorylation of tubulin by cyclin-dependent kinase 1 [10].

In this study, we identified β-tubulin as a novel DAPK2-interacting partner using pull-down assays and mass spectrometry (MS). DAPK2 strongly interacted with tubulin during nocodazole-induced apoptosis. Furthermore, we found that DAPK2 knockdown resulted in a significant suppression of nocodazole-induced apoptotic cell death. These findings indicate that DAPK2 mediates nocodazole-induced apoptosis through interaction with tubulin.

2. Materials and methods

2.1. Antibodies

Antibody against DAPK2 was purchased from Millipore, and anti-Strep antibody was purchased from Qiagen. Anti-FLAG M2 antibody was purchased from Sigma. Anti-α-tubulin and anti-pan-14-3-3 antibodies were from Santa Cruz Biotechnology. Anti-PARP antibody and anti-14-3-3 ζ/δ antibodies were from Cell Signaling Technology, and anti-glutathione S-transferase (GST) and anti-β-tubulin antibodies were from Wako Pure Chemical Industries.

2.2. Plasmid construction

The expression plasmids pFLAG-DAPK2 and p105-DAPK2 encoding mouse DAPK2 are previously described [7,11]. Full-length human β-tubulin cDNA was cloned by PCR using specific primers. The PCR product was cloned into the TA-cloning vector pGEM-T Easy (Promega), and the inserted DNA sequences were confirmed by DNA sequencing. The full-length β-tubulin cDNA was subcloned into the mammalian expression vectors pFLAG-CMV-2 (Sigma) and pEXPR-IBA105 (IBA). Site-directed mutagenesis was performed using the PrimeSTAR Mutagenesis Basal Kit (TaKaRa Bio) according to the manufacturer's instructions. The mutation was confirmed by DNA sequencing analysis.

2.3. Cell culture, transfection, and RNA interference

HeLa and HEK293T cells were cultured in Dulbecco's modified Eagle's medium supplemented with 10% fetal bovine serum, 100 units/ml penicillin, and 100 μg/ml streptomycin at 37 °C in 5% CO_2. Transfection and RNA interference were performed using Lipofectamine 2000 (Invitrogen) according to the manufacturer's instructions. The synthetic small interfering RNA (siRNA) oligonucleotide for DAPK2 was purchased from Sigma (ID# SASI_Hs01_00206405). MISSION siRNA Universal Negative Control #1 (Sigma) was used as the negative control. Nocodazole treatment was performed after 24 h of transfection or knockdown.

2.4. Protein identification by matrix-assisted laser desorption/ionization time-of-flight mass spectrometry

HeLa cells were transfected with p105-DAPK2. After 24 h, the cells were scraped in cell lysis buffer (20 mM Tris–HCl, pH 7.5, 150 mM NaCl, 0.5% NP-40, 1 mM EDTA, 10 mM leupeptin, and 10 mg/ml aprotinin). The cell extracts were centrifuged at 10,000 × g for 10 min at 4 °C, and the supernatants were incubated with Strep-Tactin Sepharose (IBA) overnight at 4 °C. The beads were washed with wash buffer (20 mM Tris–HCl, pH 7.5, 150 mM NaCl, 0.1% NP-40, and 1 mM EDTA), and the bound proteins were eluted with 6× SDS-loading buffer. The eluates were resolved by 10% SDS-PAGE, followed by silver staining (Silver Staining MS Kit; Wako Pure Chemical Industries). The subsequent protocol has previously been described [7]. Briefly, the bands in the gel were cut off and destained. After the protein bands were reduced and alkylated by dithiothreitol and iodoacetamide, respectively, trypsin digestion was performed overnight at 37 °C. The trypsin-digested peptides were extracted and desalted using C18 ZipTip (Millipore). The samples were mixed with the matrix, and then spotted onto the AnchorChip sample target (Bruker Daltonics). The mass spectra of the peptides were acquired by matrix-assisted laser desorption/ionization time-of-flight mass spectrometry (MALDI-TOF MS) (Autoflex Speed; Bruker Daltonics) and processed using FlexAnalysis 3.3 and Biotools 3.2 (Bruker Daltonics). The generated data were analyzed using the Mascot Server (Matrix Science).

2.5. Co-immunoprecipitation and pull-down assays

For the Strep or GST pull-down assays, HEK293T or HeLa cells were co-transfected with DAPK2 and β-tubulin. After 24 h, the cells were scraped in lysis buffer, and the cell lysates were incubated with Strep-Tactin or Glutathione Sepharose overnight at 4 °C. The bound proteins were analyzed by immunoblot analysis using anti-FLAG M2 antibody, anti-Strep antibody, and/or anti-GST antibody.

2.6. Apoptotic cell death assay

Apoptotic cell death was evaluated using Cell Death Detection ELISA (Roche) according to the manufacturer's instructions. After 24 h of nocodazole treatment, the cells were harvested with incubation buffer. After centrifugation, the cell lysates were added to a 96-well plate coated with anti-histone antibody. Following washing with wash buffer, a peroxidase-conjugated anti-DNA antibody was added to each well. After washing, 2,2′-azino-bis(3-ethylbenzthiazoline)-6-sulfonic acid substrate solution for peroxidase was added to generate a colored reaction product. The absorbance of the samples was determined using the Infinite M200 plate reader (Tecan) at 405 nm.

2.7. Statistical analysis

All experiments were performed multiple times to confirm their reproducibility. One representative set of data was shown in the figures. The results were quantified using Image J software (NIH). Data were expressed as the mean ± standard error, and statistical analysis was performed by one-way analysis of variance (ANOVA) with Tukey's multiple comparison test using GraphPad Prism (GraphPad Software).

3. Results

3.1. Identification of β-tubulin as a novel binding partner to DAPK2

To understand the molecular mechanisms underlying DAPK2-induced apoptosis, we attempted to identify novel binding partners of DAPK2. We previously identified 14-3-3 proteins as the interaction partners of DAPK2 from human breast cancer MCF-7 cells by combined Strep pull-down assay and MALDI-TOF MS,

which shows that this approach is very useful for the identification of interacting proteins [7]. In the present study, the Strep pull-down assay was performed using human cervical epithelial HeLa cells instead of MCF-7 cells. HeLa cells endogenously express DAPK2 protein (Fig. 1D), and a previous report has shown that the overexpression of constitutively active DAPK2 in HeLa cells induces apoptosis [12]. Furthermore, because HeLa cells can be transiently transfected with high efficiency and high expression levels compared with MCF-7 cells, we expected to identify novel DAPK2-interacting proteins. After transfection into HeLa cells with Strep-tagged DAPK2, the cell lysates were subjected to Strep pull-down assay, followed by SDS-PAGE and silver staining. As shown in Fig. 1A, the specific protein bands at 30, 31, 44, 55, and 88 kDa were found in the precipitates from cells transfected with Strep–DAPK2 compared with those from control cells. The bands at 44 and 88 kDa were close to the molecular masses of the Strep–DAPK2 and its SDS-resistant dimer, respectively, while the two bands at 30 and 31 kDa were 14-3-3 proteins in accordance with our previous study [7]. Therefore, the 55-kDa band was excised and analyzed by MALDI-TOF MS after in-gel tryptic digestion. The analysis revealed that the 55-kDa protein was β-tubulin. To confirm the interaction between DAPK2 and β-tubulin, we performed a Strep pull-down assay using lysates prepared from HEK293T cells expressing Strep–DAPK2 and FLAG-tagged β-tubulin. As shown in Fig. 1B, Strep–DAPK2 specifically interacted with FLAG–β-tubulin.

In cells, most β-tubulin forms a heterodimer with α-tubulin. Therefore, we next investigated the interaction between DAPK2 and α-tubulin. HEK293T cells were transfected with either Strep–DAPK2 or Strep empty vector. After the Strep pull-down assay, the precipitated proteins were analyzed by western blotting with anti-α-tubulin antibody. As shown in Fig. 1C, Strep–DAPK2 interacted with not only β-tubulin but also α-tubulin, indicating that DAPK2 interacts with the α/β-tubulin heterodimer. Furthermore, we examined the endogenous interaction between DAPK2 and β-tubulin. Endogenous expression of DAPK2 protein in HeLa cells was confirmed by knockdown analysis using siRNA (Fig. 1D). Subsequently, we performed immunoprecipitation using the cell lysates from HeLa cells, followed by western blotting with anti-β-tubulin antibody. β-Tubulin was detected when the cell lysates were immunoprecipitated with anti-DAPK2 antibody (Fig. 1D, *IP: DAPK2*). In contrast, control IgG did not precipitate β-tubulin (Fig. 1D, *IP: IgG*). These results support that DAPK2 and β-tubulin are physiologically interacting partners.

3.2. β-Tubulin interacts with monomeric but not dimeric DAPK2

To identify the region of DAPK2 that interacts with β-tubulin, we produced deletion mutants of DAPK2, the DAPK2 catalytic domain (DAPK2 CD) and the C-terminal region lacking the catalytic domain (DAPK2 ΔCD) (Fig. 2A). We performed GST pull-down assays using these mutants. As shown in Fig. 2B, we confirmed that GST-fused full-length DAPK2 (GST–DAPK2 WT) interacted with Strep-tagged β-tubulin. Although DAPK2 ΔCD could bind to β-tubulin, DAPK2 CD could not, suggesting that DAPK2 interacts with β-tubulin via its C-terminal region (amino acids 288–370). The C-terminal region of DAPK2 mediates its homodimer formation [13,14], and additionally contains the 14-3-3-binding region [7,15]. We considered that the interaction between DAPK2 and β-tubulin may influence the homodimer formation and/or 14-3-3 interaction. Thus, we prepared two FLAG-tagged DAPK2 mutants (DAPK2 Δ367 and DAPK2 T369A). The DAPK2 Δ367 mutant cannot form a homodimer nor interact with 14-3-3 proteins, and the DAPK2 T369A mutant only weakly binds to 14-3-3 proteins [7]. Using Strep pull-down assays, we analyzed the binding of Strep–β-tubulin to these mutants. Although FLAG–DAPK2 wild type (FLAG–DAPK2 WT) formed a homodimer, Strep–β-tubulin specifically interacted only with monomeric DAPK2 (Fig. 2C). On the other hand, DAPK2 Δ367 and DAPK2 T369A displayed no or little dimerization and binding to β-tubulin. These results suggest that the binding of dimeric DAPK2 to tubulin is interfered by its conformation and/or other binding

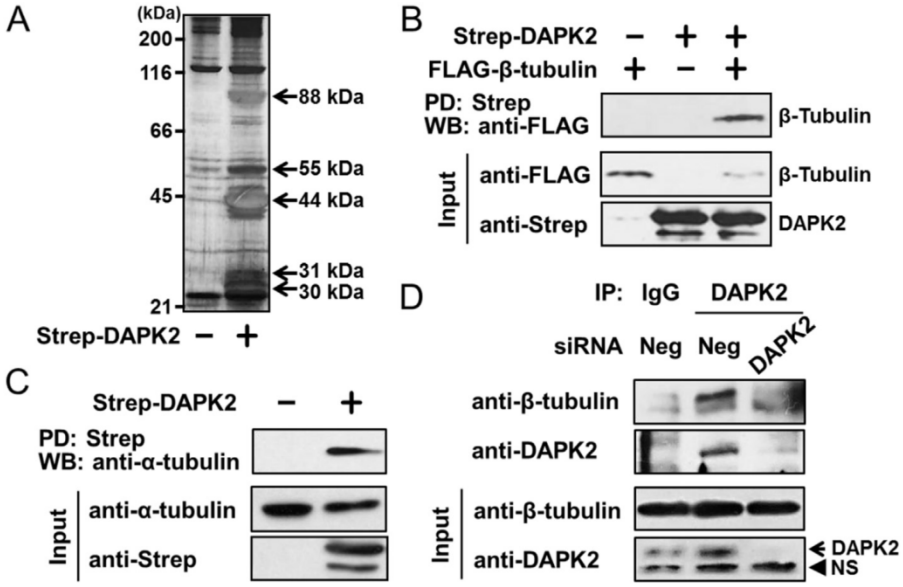

Fig. 1. Identification of β-tubulin as a binding protein for DAPK2. (A) HeLa cells were transfected with either Strep empty vector or Strep–DAPK2. After 24 h, the cells were scraped in lysis buffer, and were used in a Strep pull-down assay. The bound proteins were resolved by SDS-PAGE, followed by silver staining. (B and C) HEK293T cells were transfected with Strep–DAPK2 with or without FLAG–β-tubulin. The cell lysates were pulled down with Strep-Tactin (*PD: Strep*), followed by western blotting with anti-FLAG (B, *WB: anti-FLAG*) or anti-α-tubulin antibodies (C, *WB: anti-α-tubulin*). Protein expression was confirmed by western blotting the total cell lysates (*Input*). (D) HeLa cells were transfected with siRNA against DAPK2 or negative control siRNA (*Neg*). The cell lysates were immunoprecipitated using either anti-DAPK2 antibody (*IP: DAPK2*) or normal rabbit IgG (*IP: IgG*). The immunoprecipitates were analyzed by western blotting with anti-β-tubulin or anti-DAPK2 antibodies. The endogenous expression of β-tubulin and DAPK2 was confirmed by western blotting HeLa cell lysates with the appropriate antibodies (*Input*). NS indicates a nonspecific band. All experiments were performed multiple times with similar results.

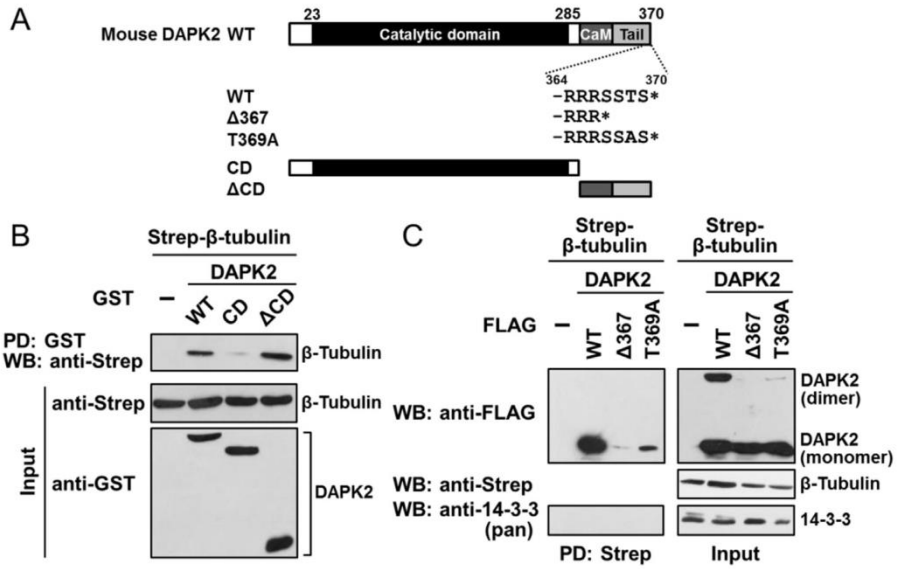

Fig. 2. β-Tubulin interacts with the C-terminal region of DAPK2. (A) Schematic representations of DAPK2 and its mutants are shown. (B) Strep–β-tubulin was co-expressed with GST–DAPK2 wild type (*WT*) or its deletion mutants (DAPK2 CD and DAPK2 ΔCD) in HEK293T cells. The cell lysates were pulled down with Glutathione Sepharose and analyzed by western blotting with anti-Strep antibody. (C) HEK293T cells were transfected with FLAG–DAPK2 wild type (*WT*) or its mutants together with Strep–β-tubulin. The cell lysates were pulled down with Strep-Tactin (*PD: Strep*), followed by western blotting with anti-FLAG or anti-pan-14-3-3 antibodies. Protein expression was confirmed by western blotting the total cell lysates with the appropriate antibodies (*Input*). All experiments were performed multiple times with similar results.

proteins, although the C-terminus of DAPK2 is required for the interaction with β-tubulin. In addition, although we examined the binding of the DAPK2/β-tubulin complex to 14-3-3 proteins, the interaction could not be detected (Fig. 2C), indicating that 14-3-3 proteins may not be able to recognize the DAPK2/β-tubulin complex.

3.3. *DAPK2 is partially required for nocodazole-induced apoptosis*

Because microtubule dynamics play an important role in many cellular functions, their disruption results in apoptotic cell death. Nocodazole has long been used as a standard microtubule depolymerizing agent and causes apoptosis in various types of cells. Therefore, we investigated whether DAPK2 is involved in nocodazole-induced apoptosis. In apoptotic cells, poly (ADP-ribose) polymerase (PARP) (116 kDa) is cleaved by caspases into 89- and 25-kDa fragments [16]. We examined the level of an apoptotic marker, cleaved PARP, by western blotting with an antibody that recognizes both the 116-kDa intact form and the 89-kDa fragment of PARP. Treatment of HeLa cells with nocodazole (0.1 and 1 μg/ml) led to approximately five-fold increases in the ratio of cleaved PARP-to-uncleaved PARP (Fig. 3A), confirming that nocodazole induces apoptosis in HeLa cells. In DAPK2 knockdown cells, the cleavage of PARP triggered by nocodazole (1 μg/ml) was significantly but not completely decreased. These results were further confirmed using another apoptosis assay that measures cytoplasmic histone-associated DNA fragments (Fig. 3B), indicating that DAPK2 partially mediates nocodazole-induced apoptosis.

Finally, we investigated whether the DAPK2–tubulin interaction is associated with nocodazole-induced apoptosis. HEK293T cells transfected with either Strep–DAPK2 or Strep empty vector together with FLAG-β-tubulin were treated with 1 μg/ml nocodazole, followed by the Strep pull-down assay. As shown in Fig. 4A, the DAPK2–tubulin interaction was extremely enhanced by nocodazole treatment. Furthermore, we also explored whether the association between DAPK2 and 14-3-3 proteins is affected by nocodazole. When HeLa cells transfected with Strep-DAPK2 were treated with nocodazole, the interaction between DAPK2 and 14-3-3 proteins was markedly reduced compared with no treatment (Fig. 4B). These results indicate that the nocodazole treatment enables DAPK2 to release from 14-3-3 proteins and interact with α/β-tubulin heterodimers.

4. Discussion

Although the members of the DAPK family show high homology in the N-terminal catalytic domain, the C-terminal regulatory domains differ from each other. Therefore, the differences in the physiological functions of the DAPK family members are thought to be due to these variations in the C-terminal regions, which correspondingly result in different interacting partners and/or specific subcellular localizations. The C-terminal region of DAPK2 contains a CaM-binding domain and a 40-amino acid C-terminal tail that shows no homology to the other DAPK family members and mediates its homodimerization. Moreover, our and others recent studies [7,15] showed that 14-3-3 proteins bind to the serine/threonine-rich sequence in the C-terminal tail of DAPK2 in a phosphorylation-dependent manner and suppress its kinase activity and subsequent apoptosis, suggesting the unique regulation of DAPK2 by 14-3-3 proteins. In the present study, we identified β-tubulin as a novel DAPK2-interacting partner in HeLa cells using a combined pull-down assay and MS approach. Monomeric but not dimeric DAPK2 bound to α/β-tubulin heterodimers via its unique C-terminal region. Because structural analysis indicated that the monomerization of DAPK2 is necessary for enzymatic activation [14], we suggested that monomeric DAPK2 bound to tubulin is enzymatically active. Thus, the involvement of DAPK2 in microtubule disruption-induced apoptosis was investigated. Although the microtubule polymerization inhibitor nocodazole, which elevates intracellular Ca^{2+} concentration [17], induced apoptosis, siRNA-mediated silencing of DAPK2 significantly suppressed the induction of apoptosis. In addition, nocodazole decreased the formation of the DAPK2/14-3-3 complex, while it promoted the formation of the DAPK2/tubulin complex. DAPK2 phosphorylated by the survival

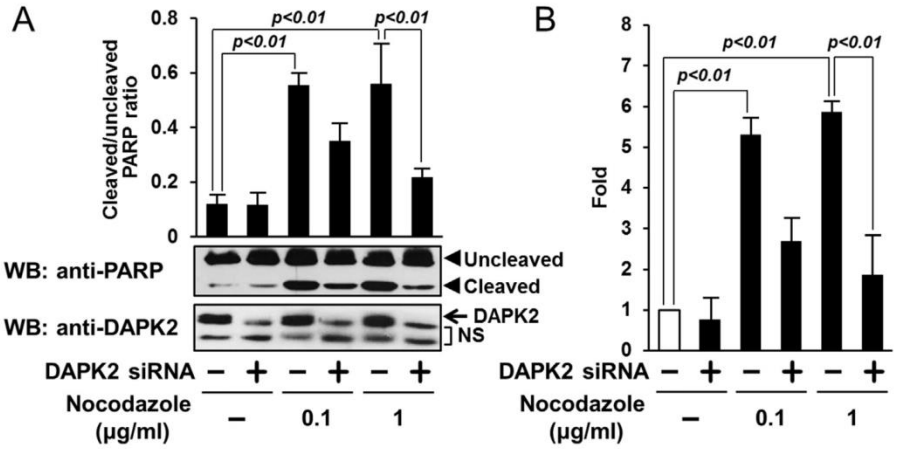

Fig. 3. DAPK2 partially mediates nocodazole-induced apoptosis. (A) HeLa cells were transfected with DAPK2 siRNA or negative control siRNA. After 24 h of transfection, the cells were treated with 0.1 or 1 μg/ml nocodazole or DMSO as a control for 24 h. The total cell lysates were subsequently analyzed by western blotting with anti-PARP or anti-DAPK2 antibodies. The bands of cleaved and uncleaved PARP were quantitated using Image J software. The ratio of cleaved PARP-to-uncleaved PARP is shown in the graph. The results are expressed as the mean ± standard error of three independent experiments, and statistical analysis was performed by one-way ANOVA with Tukey's multiple comparison test. *NS* indicates a nonspecific band. (B) HeLa cells transfected with DAPK2 siRNA or negative control siRNA were exposed to DMSO (control, −) or nocodazole (0.1 and 1 μg/ml) for 24 h. The cytoplasmic histone-associated DNA fragments were quantitatively determined using the Cell Death Detection ELISA Kit. The results are expressed as the fold induction relative to the values obtained from the negative control siRNA-transfected cells treated with DMSO (*open bar*). The data are presented as the mean ± standard error derived from three independent experiments, and statistical analysis was performed by one-way ANOVA with Tukey's multiple comparison test.

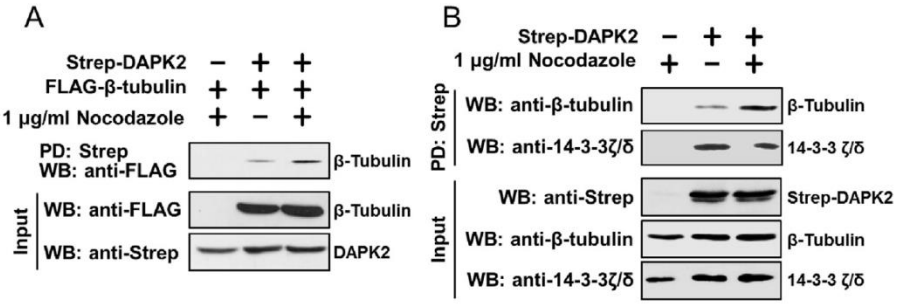

Fig. 4. Nocodazole promotes the interaction of DAPK2 with tubulin. (A) HEK293T cells transfected with Strep–DAPK2 in combination with FLAG–β-tubulin were treated with 1 μg/ml nocodazole or DMSO as a control for 10 h. The cell lysates were used for Strep pull-down assays, and the protein expression was confirmed by western blotting with the appropriate antibodies. The data are expressed as the fold induction relative to the values obtained from DMSO-treated cells (nocodazole (−), *open bar*). (B) HeLa cells transfected with either Strep empty vector or Strep–DAPK2 were treated with 1 μg/ml nocodazole or DMSO as a control for 4 h. After the Strep pull-down, the precipitated samples were analyzed by western blotting analysis using anti-β-tubulin and anti-14-3-3 ζ/δ antibodies. All experiments were performed multiple times with similar results.

kinase Akt is associated with 14-3-3 proteins in growing cells, whereas the Ca^{2+}/CaM-regulated protein phosphatase calcineurin dephosphorylates DAPK2, resulting in its dissociation from 14-3-3 proteins [7]. Taken together, it is suggested that monomeric DAPK2 released from 14-3-3 proteins by nocodazole treatment binds to α/β-tubulin heterodimers and induces apoptotic cell death, possibly via the phosphorylation of the proteins that regulate microtubule dynamics.

The dynamics of microtubules, which are composed of α/β-tubulin heterodimers, are regulated by microtubule-stabilizing and microtubule-destabilizing factors. Although the phosphorylation of these factors contributes to the regulation of microtubule dynamics, phosphorylation of tubulin itself is also involved. Cyclin-dependent kinase 1 phosphorylates β-tubulin, and phosphorylated β-tubulin regulates microtubule dynamics during mitosis [10]. Therefore, we examined whether DAPK2 also phosphorylates β-tubulin. However, an *in vitro* kinase assay revealed that DAPK2 failed to phosphorylate β-tubulin, although myosin light chain 2, which is an established substrate for DAPK2, was phosphorylated (data not shown). On the other hand, DAPK1 regulates the microtubule-associated protein tau through tau Thr^{231} and Pin1 phosphorylation, resulting in the inhibition of microtubule assembly [18]. DAPK1 inhibits the prolyl isomerase activity of Pin1 by phosphorylating Ser^{71} (-QSRRPS^{71}S) [19]. A more recent study showed that the phospho-RXRXXpS/T antibody could detect a binding partner of target of rapamycin, raptor, when it was phosphorylated by DAPK2 [20], suggesting that DAPK2 may specifically recognize and phosphorylate the RXXpS/T sequence. DAPK2 may also regulate microtubule-associated proteins, including tau, via phosphorylation of Pin1 at Ser^{71}, leading to the regulation of microtubule dynamics.

In conclusion, we identified tubulin as an interacting partner of DAPK2. DAPK2 is involved in nocodazole-induced apoptosis (possibly via the regulation of microtubule dynamics). Further studies on not only interacting partners but also substrates of DAPK2 will elucidate the molecular mechanisms underlying DAPK2-induced apoptosis.

Acknowledgments

The authors thank Ms. Yuka Sasaki for her technical assistance. This study was supported in part by Grant-in-Aid for Japan Society

for the Promotion of Science (JSPS) Fellows (13J08248) (K. Isshiki) and by a grant from the Awa Bank Science and Culture Foundation of Tokushima (K. Yuasa).

Transparency document

Transparency document related to this article can be found at http://dx.doi.org/10.1016/j.bbrc.2015.10.151.

References

[1] D. Gozuacik, A. Kimchi, DAPk protein family and cancer, Autophagy 2 (2006) 74–79.
[2] R. Shiloh, S. Bialik, A. Kimchi, The DAPK family: a structure-function analysis, Apoptosis 19 (2014) 286–297.
[3] C.R. Schlegel, A.V. Fonseca, S. Stöcker, M.L. Georgiou, M.B. Misterek, C.E. Munro, C.R. Carmo, M.J. Seckl, A.P. Costa-Pereira, DAPK2 is a novel modulator of TRAIL-induced apoptosis, Cell Death Differ. 21 (2014) 1780–1791.
[4] W.J. Wang, J.C. Kuo, C.C. Yao, R.H. Chen, DAP-kinase induces apoptosis by suppressing integrin activity and disrupting matrix survival signals, J. Cell Biol. 159 (2002) 169–179.
[5] C.C. Chang, M.H. Yang, B.R. Lin, S.T. Chen, S.H. Pan, M. Hsiao, T.C. Lai, S.K. Lin, Y.M. Jeng, C.Y. Chu, R.H. Chen, P.C. Yang, Y.E. Chin, M.L. Kuo, CCN2 inhibits lung cancer metastasis through promoting DAPK-dependent anoikis and inducing EGFR degradation, Cell Death Differ. 20 (2013) 443–455.
[6] T. Usui, M. Okada, H. Yamawaki, Zipper interacting protein kinase (ZIPK): function and signaling, Apoptosis 19 (2014) 387–391.
[7] K. Yuasa, R. Ota, S. Matsuda, K. Isshiki, M. Inoue, A. Tsuji, Suppression of death-associated protein kinase 2 by interaction with 14-3-3 proteins, Biochem. Biophys. Res. Commun. 464 (2015) 70–75.
[8] P. Singh, K. Rathinasamy, R. Mohan, D. Panda, Microtubule assembly dynamics: an attractive target for anticancer drugs, IUBMB Life 60 (2008) 368–375.
[9] C. Dong, Z. Li, R. Alvarez Jr., X.H. Feng, P.J. Goldschmidt-Clermont, Microtubule binding to Smads may regulate TGFβ activity, Mol. Cell 5 (2000) 27–34.
[10] A. Fourest-Lieuvin, L. Peris, V. Gache, I. Garcia-Saez, C. Juillan-Binard, V. Lantez, D. Job, Microtubule regulation in mitosis: tubulin phosphorylation by the cyclin-dependent kinase Cdk1, Mol. Biol. Cell. 17 (2006) 1041–1050.
[11] K. Isshiki, S. Matsuda, A. Tsuji, K. Yuasa, cGMP-dependent protein kinase I promotes cell apoptosis through hyperactivation of death-associated protein kinase 2, Biochem. Biophys. Res. Commun. 422 (2012) 280–284.
[12] B. Inbal, S. Bialik, I. Sabanay, G. Shani, A. Kimchi, DAP kinase and DRP-1 mediate membrane blebbing and the formation of autophagic vesicles during programmed cell death, J. Cell Biol. 157 (2002) 455–468.
[13] G. Shani, S. Henis-Korenblit, G. Jona, O. Gileadi, M. Eisenstein, T. Ziv, A. Admon, A. Kimchi, Autophosphorylation restrains the apoptotic activity of DRP-1 kinase by controlling dimerization and calmodulin binding, EMBO J. 20 (2001) 1099–1113.
[14] A.K. Patel, R.P. Yadav, V. Majava, I. Kursula, P. Kursula, Structure of the dimeric autoinhibited conformation of DAPK2, a pro-apoptotic protein kinase, J. Mol. Biol. 409 (2011) 369–383.
[15] Y. Gilad, R. Shiloh, Y. Ber, S. Bialik, A. Kimchi, Discovering protein-protein interactions within the programmed cell death network using a protein-fragment complementation screen, Cell Rep. 8 (2014) 909–921.
[16] M. Tewari, L.T. Quan, K. O'Rourke, S. Desnoyers, Z. Zeng, D.R. Beidler, G.G. Poirier, G.S. Salvesen, V.M. Dixit, Yama/CPP32 beta, a mammalian homolog of CED-3, is a CrmA-inhibitable protease that cleaves the death substrate poly(ADP-ribose) polymerase, Cell 81 (1995) 801–809.
[17] S.L. Mironov, M.V. Ivannikov, M. Johansson, $[Ca^{2+}]_i$ signaling between mitochondria and endoplasmic reticulum in neurons is regulated by microtubules from mitochondrial permeability transition pore to Ca^{2+}-induced Ca^{2+} release, J. Biol. Chem. 280 (2005) 715–721.
[18] B.M. Kim, M.H. You, C.H. Chen, S. Lee, Y. Hong, Y. Hong, A. Kimchi, X.Z. Zhou, T.H. Lee, Death-associated protein kinase 1 has a critical role in aberrant tau protein regulation and function, Cell Death Dis. 5 (2014) e1237.
[19] T.H. Lee, C.H. Chen, F. Suizu, P. Huang, C. Schiene-Fischer, S. Daum, Y.J. Zhang, A. Goate, R.H. Chen, X.Z. Zhou, K.P. Lu, Death-associated protein kinase 1 phosphorylates Pin1 and inhibits its prolyl isomerase activity and cellular function, Mol. Cell 44 (2011) 147–159.
[20] Y. Ber, R. Shiloh, Y. Gilad, N. Degani, S. Bialik, A. Kimchi, DAPK2 is a novel regulator of mTORC1 activity and autophagy, Cell Death Differ. 22 (2015) 465–475.